

# Journal Pre-proof

A non-metal Acen-H catalyst for the chemical fixation of CO<sub>2</sub> into cyclic carbonates under solvent- and halide-free mild reaction conditions

Zhongxiao Yue (Conceptualization) (Investigation) (Methodology) (Formal analysis) (Data curation) (Writing - original draft), Manoj Pudukudy (Writing - review and editing) (Supervision) (Funding acquisition), Shiyu Chen (Writing - review and editing), Yi Liu (Writing - review and editing), Wenbo Zhao (Writing - review and editing), Junya Wang (Writing - review and editing), Shaoyun Shan (Resources) (Writing - review and editing) (Supervision) (Funding acquisition) (Project administration), Qingming Jia (Resources) (Writing - review and editing)



PII: S0926-860X(20)30239-8

DOI: <https://doi.org/10.1016/j.apcata.2020.117646>

Reference: APCATA 117646

To appear in: *Applied Catalysis A, General*

Received Date: 14 March 2020

Revised Date: 12 May 2020

Accepted Date: 18 May 2020

Please cite this article as: Yue Z, Pudukudy M, Chen S, Liu Y, Zhao W, Wang J, Shan S, Jia Q, A non-metal Acen-H catalyst for the chemical fixation of CO<sub>2</sub> into cyclic carbonates under solvent- and halide-free mild reaction conditions, *Applied Catalysis A, General* (2020), doi: <https://doi.org/10.1016/j.apcata.2020.117646>

This is a PDF file of an article that has undergone enhancements after acceptance, such as the addition of a cover page and metadata, and formatting for readability, but it is not yet the definitive version of record. This version will undergo additional copyediting, typesetting and review before it is published in its final form, but we are providing this version to give early visibility of the article. Please note that, during the production process, errors may be discovered which could affect the content, and all legal disclaimers that apply to the journal pertain.

© 2020 Published by Elsevier.

# A non-metal Acen-H catalyst for the chemical fixation of CO<sub>2</sub> into cyclic carbonates under solvent- and halide-free mild reaction conditions

Zhongxiao Yue <sup>a</sup>, Manoj Pudukudy <sup>a,b</sup>, Shiyu Chen <sup>a</sup>, Yi Liu <sup>a</sup>, Wenbo Zhao <sup>a</sup>, Junya Wang <sup>b</sup>,  
Shaoyun Shan <sup>a,\*</sup>, Qingming Jia <sup>a,1</sup>

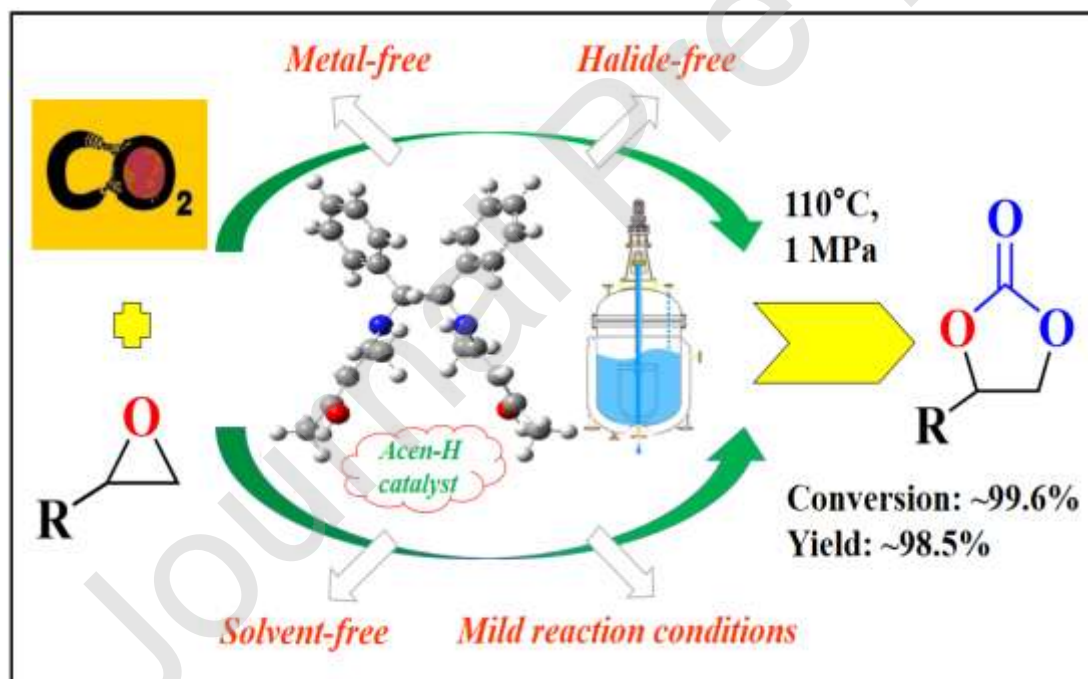
<sup>a</sup> Faculty of Chemical Engineering, Kunming University of Science and Technology, Kunming,  
Yunnan, 650500, China

<sup>b</sup> Faculty of Environmental Science and Engineering, Kunming University of Science and  
Technology, Kunming, Yunnan, 650500, China

\*Email: [huagong327@163.com](mailto:huagong327@163.com); [shansy411@163.com](mailto:shansy411@163.com)

(<sup>1</sup> Deceased author, Date of Death: 25<sup>th</sup> November 2019)

## Graphical Abstract



## Highlights

- A metal-free Acen-H catalyst was successfully synthesized by a single step reflux method.

- The Acen-H catalyst exhibited high catalytic activity for the cycloaddition of CO<sub>2</sub> with epichlorohydrin.
- The reactions were performed in a solvent- and halide-free reaction condition.
- High epoxide conversion and product selectivity & yield were achieved at 1.0 MPa and 110 °C.
- A plausible reaction mechanism validated through DFT simulation was proposed.

## Abstract

A metal-free Acen-H catalyst was effectively synthesized by a single step reflux method and successfully tested for the cycloaddition of CO<sub>2</sub> with epoxides to synthesize cyclic carbonates. The Acen-H catalyst exhibited high activity and selectivity for the cycloaddition reaction in the absence of co-catalysts (halides) and solvents at mild reaction conditions of a reaction temperature of 110 °C and a reaction pressure of 1 MPa. Under the optimized reaction conditions, most of the epoxides were successfully converted into corresponding cyclic carbonates with a highest yield of ~98.5%. The composition and structure of the homogeneous catalyst was then systematically evaluated and the reaction kinetics and a plausible reaction mechanism for the cycloaddition of CO<sub>2</sub> with epoxides were proposed. The density functional theory (DFT) calculation provided a corroborated elucidation for the proposed mechanism. The catalytic activity of the Acen-H catalyst was found to be originated from the active hydrogen bond donors (-O-H, =N---H) and imino groups present (-N=) in it, which played a synergistic role in the adsorption and activation of reactants as confirmed by the DFT studies. The structural characteristics of the catalyst was found to be crucial for the cycloaddition of CO<sub>2</sub> with epoxides.

**Keywords:** CO<sub>2</sub> conversion; Cycloaddition; Cyclic carbonates; Acen-H catalyst; Metal-free catalysis; Reaction kinetics

## 1. Introduction

Due to carbon dioxide's (CO<sub>2</sub>) impact on global warming, the increased emission of CO<sub>2</sub> has become a major environmental problem, which is recognized by the international community [1].

---

This fact has become a vital driving force for the reduction of greenhouse gas emission for the development of a sustainable environment. With an emphasis on the carbon oxides-based pollution and the development of synthetic fuel chemistry, the utilization of CO<sub>2</sub> has attracted much attention in academia and industrial chemists [2]. The environmental impacts of CO<sub>2</sub> can be minimized by its utilization as it can be chemically fixed into highly value-added products and fuels [3]. Among them, cyclic carbonates [4, 5] and polycarbonates [6, 7] are the successful examples of chemically fixed CO<sub>2</sub>.

Currently, there are different ways to synthesize cyclic carbonates from CO<sub>2</sub>. It includes the chemical reaction of CO<sub>2</sub> with different compounds such as epoxides [4, 5], ethylene glycol and its derivatives [8, 9], etc. The selection of epoxides as highly active substrates was reported to reduce the energy demand as it overcame the thermodynamic and kinetic limitations of inert CO<sub>2</sub> [4, 10]. Therefore, the synthesis of cyclic carbonates by the ring-opening addition of CO<sub>2</sub> with epoxides is of great importance, which owns the characteristics of simple synthesis and cost-effectiveness without the formation of by-products. The benefits of this synthesis mainly lie on two aspects: On the one side, it adheres to the initiation of green chemistry and low carbon economy; on the other side, it can be widely applied to the production of highly value added chemicals [11, 12]. Cyclic carbonates has witnessed their valuable applications in industry, because of their unique characteristics, such as high dipole moment, boiling point, dielectric constant, stability, low toxicity, and biodegradability [13, 14]. It is widely used not only in the synthesis of fine chemical intermediates for biomedical precursors and agricultural chemicals [15], but also the synthesis of novel materials, such as heat recording materials, phenolic resins, thermosetting resins [16], polycarbonate [7], polyglycerol [17], polyurethane monomers [18], inert non-proton polar solvents [19], high energy density batteries, capacitor electrolytes [20] and so on. Therefore, the synthesis of cyclic carbonates is a hot topic in the environmental catalysis, especially, it has attracted much attention on academia and industry.

The reactions for the synthesis of cyclic carbonates from CO<sub>2</sub> and epoxides are mostly focused on the assistance of metal-based catalysts, which mainly consists of metal organic frameworks [21], metal porphyrins [22], metal oxides [23], metal ionic liquids [20] and metal Salen or Salophen complexes [4, 24, 25], etc. The metal-based homogeneous catalysts were reported to have a good solubility in the reaction mixture and exhibited high efficiency and selectivity in the ring-opening

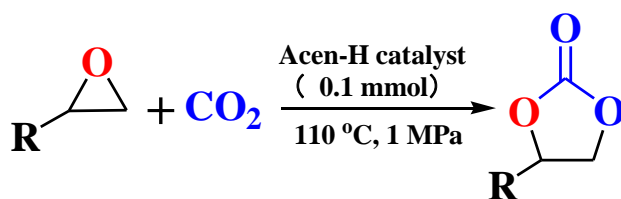
---

addition of CO<sub>2</sub> with epoxides. Some shortcomings of these homogeneous catalysts are that they would be easily degraded and inactivated in the reaction, and they would be more costly (e.g. metal based ionic liquids) [26-28]. Thus, exploiting the metal-free Schiff base catalysts is considered to be of great value in catalysis.

The Schiff base complexes have the advantages of the availability of raw materials, diverse and adjustable structure, insensitive nature to air and water, multi-functional coordination behavior, low melting point, relatively low cost and remarkable economic benefits [29-31]. However, in addition to the use of metal complexes, most of the catalytic systems have used halides as nucleophilic reagents. In the process of industrialization, there is an obvious defect that corrosiveness is caused to stainless steel reactor and other related parts [26, 32]. Therefore, it is imperative to develop highly efficient metal- and halide free Schiff base catalysts.

The catalytic reaction with metal-based catalysts has shown that the Lewis acid provides sites for the co-ordination of oxygen in the epoxides, and promotes their ring-opening under the nucleophilic attack by halides [5]. The polarization of epoxides can be generated by hydrogen bonding to some extent, and the cycloaddition gets promoted. There are many hydrogen bond donor (HBD) groups in the catalysts such as -OH [33, 34], -NH<sub>2</sub>, -COOH [35, 36] and so on. These groups can co-ordinate with the O of epoxide to form hydrogen bondings [26, 37]. Such catalysts can effectively replace the participation of metal ions, and confirm the concept of greener chemical production and the strategy of sustainability [38]. Therefore, the synthesis of catalysts for the activation and ring-opening of the substrates is a key point herein.

Based on the above viewpoints, in this study, a metal-free Schiff base homogeneous catalyst (Acen-H) was synthesized by a one-step reflux reaction by the condensation of 1,2-diphenyl-1,2-ethylenediamine with 2,4-pentanedione and their catalytic activity for the potential of cycloaddition of CO<sub>2</sub> with epoxides was explored. It exhibited remarkable catalytic performance for the carbonation reaction, especially for ring carbonation, under halide and solvent-free conditions at mild temperatures and CO<sub>2</sub> pressures (Scheme 1). Moreover, the effects of ratio of catalyst to epichlorohydrin (ECH), reaction temperature, time and initial CO<sub>2</sub> pressure on the conversion, selectivity and yield have been investigated. On the other hand, the reaction kinetics and a plausible reaction mechanism combined with the density functional theory (DFT) were reasonably explained.



**Scheme 1.** Schematic representation of the synthesis of cyclic carbonates from epoxides and  $\text{CO}_2$ .

## 2. Experimental

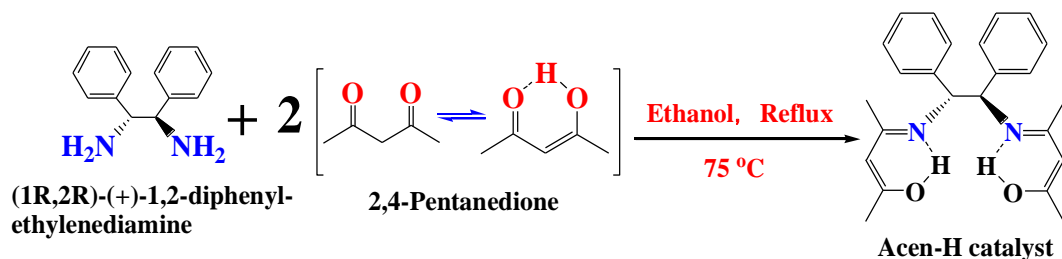
### 2.1. Materials

Salicylaldehyde (AR, 98%), (1R,2R)-(+)-1,2-diphenylethylenediamine (99%), 2,4-pentanedione (AR, 99%), 3,5-di-tert-butylsalicylaldehyde (98%), epichlorohydrin (ECH) (AR), propylene oxide (99%), ethylene oxide (99%), glycidol (96%), 1,2-butylene oxide (>99%), styrene oxide (98%), 1,2-epoxyhexane (96%), isobutylene oxide (>97%), cyclohexene oxide (98%) and chloroform-d ( $\text{CDCl}_3$ ) (D, 99.8%) were purchased from Aladdin Industrial Inc. (Shanghai, China).  $\text{CO}_2$  (99.999% purity) was purchased from Chengdu Jingkexin Gases Co., Ltd. and ethanol (AR) was obtained from Xilong Scientific Co., Ltd. (Sichuan, China). All reagents obtained from the commercial resources were used without further purification unless otherwise noted.

### 2.2. Synthesis of homogeneous Acen-H catalyst

A single step method was used to prepare the Acen-H catalyst. A solution of (1R,2R)-(+)-1,2-diphenylethylenediamine (3.1346 g, 0.0148 mol) in absolute ethanol (80 mL) was taken in a two-neck round bottom flask (250 mL) and placed in an oil bath with magnetic stirring. A reflux condenser and a separatory funnel was then placed on the above-mentioned flask. Next, 2,4-pentanedione (3.07 mL, 0.0295 mol) was dissolved in absolute ethanol (50 mL). The reaction temperature of the first mixture was increased to 75 °C, then the prepared ethanolic solution of 2,4-pentanedione was slowly added into the above solution, stirred and heated at 75 °C. The reaction was performed for 24 h unless it was noted separately. When the reaction was completed, the reaction mixture was cooled to room temperature, transferred into a one-necked flask (250 mL) and placed on a rotary evaporator to evaporate the solvents. The formed product was then transferred into a vacuum oven and dried at 55 °C for 6 h. The product obtained in the form of an amber viscous solid was named as Acen-H catalyst (VII) (Fig. 5). The schematic diagram of the synthetic route is

shown in Scheme 2. Additionally, two Salophen-H ligands (V, VI) (Fig. 5) were also prepared by the same method [39].



**Scheme 2.** Schematic representation of the synthesis of metal-free homogeneous Acen-H catalyst.

### 2.3. Characterization of the prepared samples

Fourier transform infrared spectroscopy (FT-IR) (Bruker Vertex 70 V, Germany) was used to record the FT-IR spectra of the samples in the wave number range of 4000-500  $\text{cm}^{-1}$ . The nuclear magnetic resonance ( $^1\text{H-NMR}$ ,  $^{13}\text{C-NMR}$ ) spectral analysis was carried out in a Bruker Advance III HD 600, Bruker BioSpin, Switzerland using  $\text{CDCl}_3$  as a solvent and TMS as internal standard. The elemental analysis was performed by using an Elementar Vario EL cube (EA) elemental analyzer (Elementar, Germany) to determine the elemental contents of C, H and N in the samples. The thermogravimetric analysis (TGA) was carried out in a thermal analyzer (NETZSCH TG 209F3) to study the thermal stability of the prepared sample. It was measured from room temperature to 600 $^\circ\text{C}$  with a heating rate of 10  $^\circ\text{C}/\text{min}$  in nitrogen atmosphere.

### 2.4. Catalytic performance of the prepared samples

The catalytic reactions were carried out in a high-pressure liquid phase reactor (100 mL) equipped with magnetic stirring and a temperature control. In a typical reaction, 0.1 mmol (0.0377 g) of catalyst and 50 mmol of epoxide were taken in a Teflon lined autoclave. Then,  $\text{CO}_2$  (99.999%) gas was introduced into the sealed reactor three times to remove any other gases inside the reactor. Finally, the required  $\text{CO}_2$  pressure (0.1 MPa - 3.0 MPa) was set and the reaction mixture was heated to the desired temperature (60-120  $^\circ\text{C}$ ) for a specific period of time. Once the reaction was completed, the product in the reaction vessel was allowed to cool in an ice bath and the cooled product was collected and detected by FT-IR and NMR analysis. The conversion of epoxide, product selectivity and yield were calculated using NMR peak integration method [40, 41].

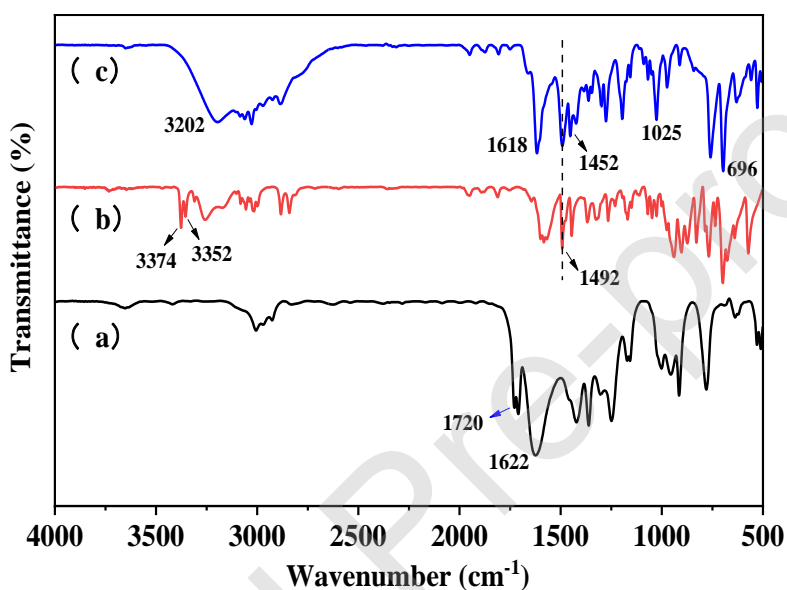
### 2.5. Density functional theory (DFT) calculation method



In order to investigate the reaction mechanism, a density functional theory (DFT) calculation was performed using Gaussian 09 program. The interactions of the equilibrium structures of the Acen-H catalyst and the substrates were obtained from the geometry optimization method by combining the standard B3LYP/6-311+G (d, p) basis set. All bond lengths were expressed in angstroms (Å) [42, 43].

### 3. Result and Discussion

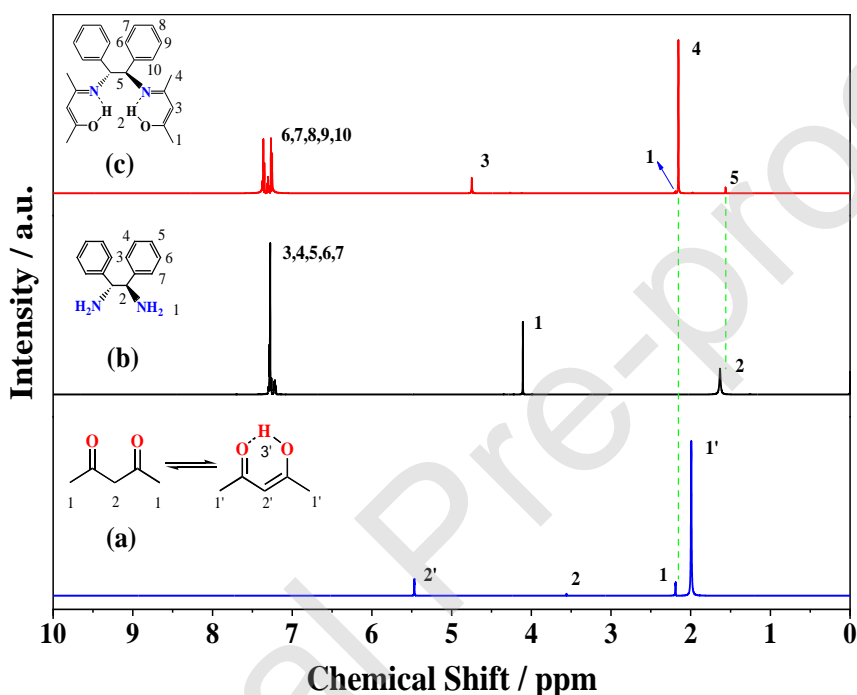
#### 3.1. Characterization of the catalysts



**Fig. 1.** FT-IR spectra of the prepared samples: (a) 2,4-pentanedione, (b) (1R,2R)-(+)-1,2-diphenylethylenediamine, (c) Acen-H catalyst.

The functional groups on the Acen-H catalyst were studied by FT-IR spectroscopy and the corresponding FT-IR spectra are shown in Fig. 1. The labels (a) and (b) represent the monomers of the Acen-H catalyst. The transmission band at  $1492\text{ cm}^{-1}$  could be attributed to the stretching vibration of the C-N bond [44]. Two transmission bands observed at  $1618\text{ cm}^{-1}$  and  $1452\text{ cm}^{-1}$  in Fig. 1(c) could be attributed to the stretching vibration of the  $>\text{C}=\text{N}$  and  $\text{C}=\text{C}$  functional groups in the prepared sample. When a conjugate structure is formed in the sample, the transmission band was found to be shifted into low frequency by  $20\text{ cm}^{-1}$  [45, 46]. The bands appeared at  $3202\text{ cm}^{-1}$  and  $696\text{ cm}^{-1}$  were attributed to the stretching and deformation vibration of the hydroxyl group respectively [47]. The band appeared at  $1025\text{ cm}^{-1}$  was due to the stretching vibration of the carbon-

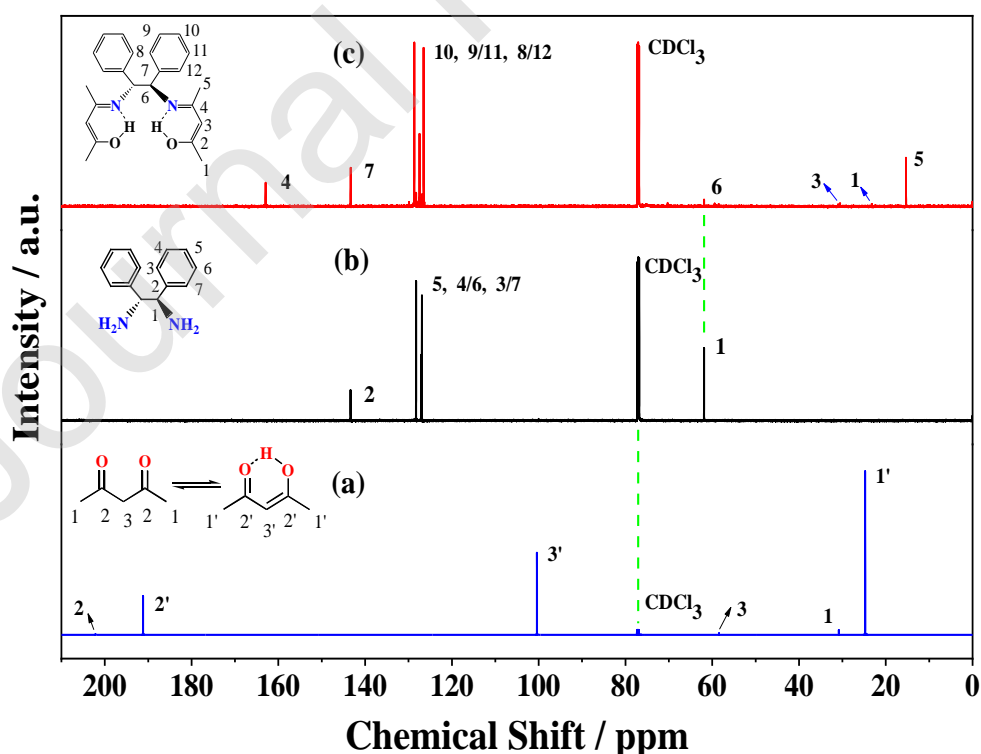
oxygen bond in the alcoholic group (C-OH). The band of  $\beta$ -diketone was not observed at  $1720\text{ cm}^{-1}$  and  $1622\text{ cm}^{-1}$  in Fig. 1(c) [48]. However, a band of hydroxyl group and a carbon-carbon double bond were observed. In addition, the transmission bands of primary amine ( $-\text{NH}_2$ ) were not seen in the Acen-H catalyst at  $3374\text{ cm}^{-1}$  and  $3353\text{ cm}^{-1}$  whereas the band of carbon-nitrogen double bond (C=N) appeared [47]. This indicates that a carbonyl group of 2,4-pentanedione and a primary amino group of (1R,2R)-(+)-1,2-diphenylethylenediamine were dehydrated to form a carbon-nitrogen double bond (C=N), i.e. secondary ketoimide.



**Fig. 2.**  $^1\text{H-NMR}$  spectra of the prepared samples: (a) 2,4-pentanedione, (b) (1R,2R)-(+)-1,2-diphenylethylenediamine, (c) Acen-H catalyst.

In order to study the structural features and changes during the catalyst synthesis, 2,4-pentanedione, (1R,2R)-(+)-1,2-diphenylethylenediamine and Acen-H catalyst were characterized by  $^1\text{H-NMR}$  spectral analysis in  $\text{CDCl}_3$  (Fig. 2). In Fig. 2(a), the tautomerism of 2,4-pentanedione composed of a ketonic and an enol configuration was presented. The enol configuration can form intramolecular hydrogen bond. The active H on the hydroxyl group is unstable, therefore it is not seen clearly in the  $^1\text{H-NMR}$  spectra and its chemical shift was about 15.4 ppm [48, 49]. The chemical shifts at 5.47 and 1.99 ppm were found in Fig. 2(a), which indicated the enol structure of

2,4-pentanedione's hydrogen atoms at H2' and H1' positions, respectively. In addition, the chemical shifts at 3.56 and 2.19 ppm with low peak intensity found in Fig. 2(a) represented the ketonic structure of 2,4-pentanedione's hydrogen atoms at H2 and H1 positions, respectively [48, 50]. In Fig. 2(b), the  $^1\text{H-NMR}$  spectra have resonances at 4.11 and 1.63 ppm, which are assigned to the hydrogen atoms (H1 and H2) of the (1R,2R)-(+)-1,2-diphenylethylenediamine, respectively. The  $^1\text{H-NMR}$  signals marked from H3 to H7 in the benzene ring were found to be located in the region of 7.32-7.22 ppm, as they are in similar chemical environment [51]. In Fig. 2(c), the chemical shifts at 4.72, 2.17, 2.12 and 1.54 ppm were corresponded to the hydrogen atoms H3, H1, H4 and H5 of the Acen-H catalyst, respectively [45, 52]. The signal of H2' in Fig. 2(a) was not positioned at the same chemical shift value in the Acen-H catalyst (Fig. 2(c)). It was appeared at 4.72 ppm. This shift could be attributed to the influence of different neighboring chemical environment [45]. The signal of H1 position at 4.11 ppm in Fig. 2(b) was not detected in Fig. 2(c), which suggests the condensation of carbonyl group (C=O) and primary amino group (-NH<sub>2</sub>) had taken place [53, 54]. By comparing with the  $^1\text{H-NMR}$  signals of (b) and (c), it was observed that the chemical shifts marked from H6 to H10 in the benzene ring of (1R,2R)-(+)-1,2-diphenylethylenediamine were observed to be shifted to 7.39-7.19 ppm (Fig. 2(c)).



**Fig. 3.**  $^{13}\text{C}$ -NMR spectra of the prepared samples: (a) 2,4-pentanedione, (b) (1R,2R)-(+)-1,2-diphenylethylenediamine, (c) Acen-H catalyst.

On the other hand, the  $^{13}\text{C}$ -NMR spectra of the 2,4-pentanedione, (1R,2R)-(+)-1,2-diphenylethylenediamine and Acen-H catalyst were characterized in  $\text{CDCl}_3$  (Fig. 3). In Fig. 3(a), the  $^{13}\text{C}$ -NMR spectra have strong resonances at 191.18, 100.40 and 24.75 ppm, which are assigned to the carbon atoms C2', C3' and C1' in enol configuration of 2,4-pentanedione, respectively [55]. Resonances at 202.16, 58.43 and 30.82 ppm were corresponded to the carbon atoms C2, C3 and C1 of ketonic configuration of 2,4-pentanedione, respectively [55]. In Fig. 3(b), the  $^{13}\text{C}$ -NMR spectra showed singlet resonance signals at 143.33 ppm. It could be attributed to the carbon atom marked as C2 and the triplet strong resonance signals at 128.26, 127.07 and 126.92 ppm were assigned to the carbon atoms C5, C4/C6, and C3/C7 in the benzene ring of (1R,2R)-(+)-1,2-diphenylethylenediamine, respectively [51]. Another strong resonance appearing at 61.88 ppm were corresponded to carbon atom C1 of (1R,2R)-(+)-1,2-diphenylethylenediamine [51]. In Fig. 3(c), the appearance of resonance signals at 162.95 ppm attributed to carbon atom C4 of the imine group moiety ( $\text{C}=\text{N}$ ) in the Acen-H catalyst [56]. In addition, the resonance signals of C2 in Fig. 3(a) was not positioned at the same chemical shift value in the Acen-H catalyst (Fig. 3(c)), which indicated that the condensation between the carbonyl groups ( $\text{C}=\text{O}$ ) of 2,4-pentanedione with the primary amino groups ( $-\text{NH}_2$ ) of (1R,2R)-(+)-1,2-diphenylethylenediamine had taken place [54]. The appearance of singlet resonance peaks at 143.34 ppm correspond to the carbon atom C7 and the triplet strong resonance peaks at 128.67, 127.47 and 126.53 ppm were assigned to the carbon atoms C10, C9/C11 and C8/C12 in benzene ring of Acen-H catalyst, respectively [51]. Other resonance signals appearing at 61.87, 30.55, 23.23 and 15.33 were assigned to the carbon atoms C6, C3, C1 and C5 of the Acen-H catalyst, respectively [51]. In particular, the chemical shifts of C3, C1 and C5 in the Acen-H catalyst shifted greatly from the corresponding carbon atoms in Fig. 3(a). Based on the above characterization results of FT-IR,  $^1\text{H}$ -NMR and  $^{13}\text{C}$ -NMR, the structure of the Acen-H catalyst is confirmed as shown in Fig.5.

The thermal stability of the Acen-H catalyst was examined by thermogravimetric analysis. The TGA-DTA curves are shown in Fig. 4. Clearly, the Acen-H catalyst exhibited two stages of weight loss. There is an initial weight loss about 6.33% in the temperature range of 35-152  $^\circ\text{C}$ , this may be

due to the loss of water molecules or other gases adsorbed on the sample. However, a sharp drop in the curve was clearly observed in the range of 154-279 °C, indicating that the catalyst had a major weight loss (about 99.60%), and its weight loss is attributed to the thermal degradation of Acen-H catalyst. However, when the temperature exceeds 280 °C, the weight loss of the Acen-H catalyst reached to zero, which indicates that the Acen-H catalyst was completely decomposed at 280 °C. Therefore, the Acen-H catalyst can be used in its stable form below this temperature for its catalytic applications.

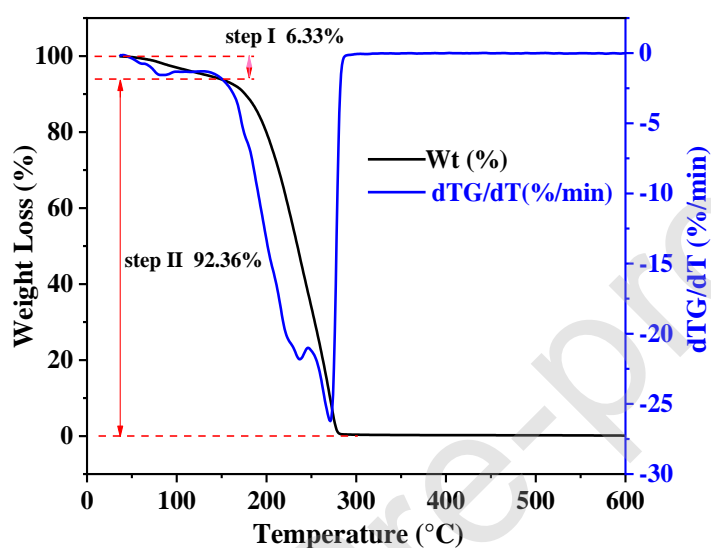


Fig. 4. TGA/DTG curves of the Acen-H catalyst.

### 3.2. Catalytic performance for cyclic carbonate synthesis

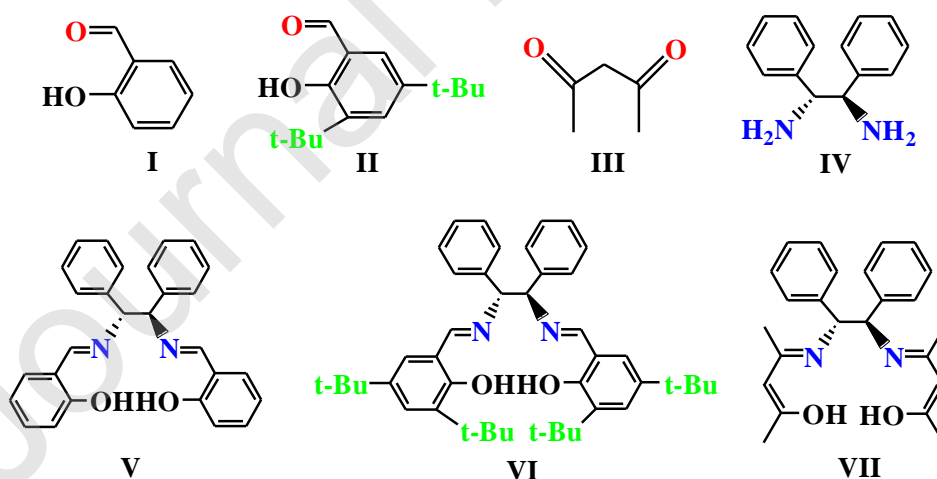


Fig. 5. Structures of the catalyst monomers (I-IV), Salophen-H ligands (V, VI) and Acen-H catalyst (VII).

In this work, we used epichlorohydrin (ECH) as a model substrate to compare the performance of the samples shown in Fig. 5 for CO<sub>2</sub> cycloaddition to prepare 3-chloropropylene carbonate, as shown in Table 1. The results show that the no conversion of ECH was observed without any catalyst (Table 1, entry 1). The precursors such as salicylaldehyde (I), 3,5-di-tert-butylsalicylaldehyde (II), 2,4-pentanedione (III), (1R,2R)-(+)-1,2-diphenylethylenediamine (IV) and Salophen-H ligands (V, VI) were found to have no effect in the reaction. However, under the same conditions, the Acen-H catalyst (VII) exhibited an ECH conversion of 99% (Table 1, entry 8). It was found that the monomers having hydroxyl, aldehydic, carbonyl or amino group could not exhibit any catalytic activity. Moreover, even the Salophen-H ligands (V, VI) and the Acen-H catalyst (VII) contains both -OH and -N=C groups, the Salophen-H ligands (V, VI) does not showed any catalytic activity, while the Acen-H catalyst (VII) showed high catalytic activity. This could be explained on the basis of high  $\pi$  delocalization effect in the Salophen-H ligands. Because of the high delocalization of  $\pi$  electrons, the O in the phenolic group will be more biased towards benzene ring [57-59] and it will be less susceptible for hydrogen bonding to activate the epoxides [26].

Additionally, the Salophen-H ligand (VI) has large steric hindrance due to t-butyl group adjacent to the phenolic group, which has an inhibitory effect on the catalytic activity [26]. Therefore, the -OH groups in the Salophen-H ligands (V, VI) were not favorable for hydrogen bonding with the oxygen of the epoxide. In the absence of metals and co-catalysts or halides, the tert-butyl groups on the ligands exhibited an inhibition in the catalytic activity for the reaction to produce cyclic carbonates [26, 60]. However, in the synthesis of polycarbonates, although the ortho substitution of tert-butyl can inhibit the catalytic activity of Salen and Salophen ligands, it can increase the solubility of the catalyst in the reaction mixture [26, 61, 62]. Moreover, it could stabilize the active metal linked to Salen and Salophen species against their decomposition in the reaction mixture for a better performance for an improved catalytic activity for the selective production of polycarbonates [60, 62, 63].

There are tautomer of enol and ketone in the Acen-H catalyst, and the enol configuration can form intramolecular hydrogen bonds [48-50]. The alcoholic group connected to the carbon-carbon double bond in the olefin has less binding with the  $\pi$  electron cloud and thereby increases the density of the -OH electron cloud [64]. Therefore, the -OH acts as a hydrogen bond donor to facilitate bonding with O in the epoxide to form a hydrogen bond and thereby polarizes the epoxide and

consequences the ring opening. In addition, the imino group in the Acen-H catalyst has a synergistic effect with -OH that also acts as a hydrogen bond donor, which enhances its catalytic performance to catalyze the cycloaddition of CO<sub>2</sub> with ECH.

**Table 1.** The results of ring-opening addition reaction of CO<sub>2</sub> and ECH under different catalysts

Entry	Catalyst	Conv. (%) <sup>[c]</sup>	Yield (%)	Select. (%)	TON <sup>[d]</sup>
1 <sup>[a], [b]</sup>	blank	Trace	0	n.d.	0
2 <sup>[a], [b]</sup>	salicylaldehyde (I)	Trace	0	n.d.	0
3 <sup>[a], [b]</sup>	3,5-di-tert-butylsalicylaldehyde (II)	Trace	0	n.d.	0
4 <sup>[a], [b]</sup>	2,4-pentanedione (III)	Trace	0	n.d.	0
5 <sup>[a], [b]</sup>	(1R,2R)-(+)-1,2-diphenylethylenediamine (IV)	Trace	0	n.d.	0
6 <sup>[a], [b]</sup>	N,N'-diphenylidene bis (salicylideneimine) (V)	Trace	0	n.d.	0
7 <sup>[a], [b]</sup>	N, N'-diphenylidene bis (3,5-di-tert-butylsalicylideneimine) (VI)	Trace	0	n.d.	0
8 <sup>[a]</sup>	N,N'-diphenylidene bis(2-hydroxy-diene deneimine) (VII)	99.0	98.5	99.4	495.2

[a] Reaction conditions: catalyst (0.1 mmol), ECH (50 mmol), temperature 110 °C, CO<sub>2</sub> pressure 1 MPa, time 4 h, 280 rpm magnetic stirring rate, [b] Reaction conditions: catalyst (0.1 mmol), ECH (10 mmol), temperature 120 °C, CO<sub>2</sub> pressure 2 MPa, time 12h, 280 rpm magnetic stirring rate, [c] Determined by <sup>1</sup>H-NMR spectroscopy using TMS as an internal standard, [d] TON (turnover number) = molar amount of initial substrate \* conversion / molar amount of catalyst.

The effects of molar ratio of ECH to Acen-H catalyst, reaction temperature, time and initial CO<sub>2</sub> pressure on the reaction efficiency were further investigated. The conversion and turnover number (TON) of ECH and the yield and selectivity of 3-chloropropylene carbonate under various reaction conditions are shown in Fig. 6. Firstly, the effect of the molar ratio of ECH to Acen-H catalyst was investigated, as shown in Fig. 6(a). We had selected mild reaction conditions, that is, the catalytic reaction was carried out at 80 °C under 1 MPa initial CO<sub>2</sub> pressure for a period of 240 min. As expected, when the molar ratio increases, the conversion and TON of ECH and the yield and selectivity of the product showed a drastic decrease. From this study, we have selected an ECH/Acen-H catalyst molar ratio of 500 for the next step, i.e. to study the effect of reaction

temperature, as shown in Fig. 6(b). With the addition of 0.1 mmol of Acen-H catalyst and an increase of the reaction temperature from 60 °C to 110 °C, the conversion was increased from 11.5% to 99.0%, the yield was increased from 10.5% to 98.5%, and the selectivity was increased from 91.3% to 99.4%, respectively, which could indicate that the catalytic reaction is an endothermic reaction and it plays an important role in the cycloaddition [2]. This might be attributed to the fact that the cyclic carbonates are thermodynamically more stable than the corresponding polycarbonates. Moreover, an increase in the reaction temperature up to an optimal level was observed to be highly beneficial for the enhancement of cyclic carbonate selectivity, as a small amount of polycarbonate was formed at low reaction temperatures. With an increase in reaction temperature, the polycarbonate is expected to be undergoing an intra-molecular ring “backbiting” mechanism, which further leads to the formation of cyclic carbonates [2, 31].

However, when the reaction temperature was increased to 120 °C, the corresponding conversion (99.2%) remained more or less same as in 110 °C, while the yield and selectivity of the product was decreased to 97.6% and 96.9%, respectively. This may be due to the formation of other by-products in the reaction such as polycarbonates, polyethers and ketones, possibly formed by the isomerization of epichlorohydrin (chloroacetone) [65, 66]. Therefore, we have selected 110 °C as the optimal temperature for the reaction giving high reactant conversion and product yield and selectivity. From this observation, we can see that increasing the temperature more than 120 °C is not worth, concerning the conversion, yield and product selectivity of the cycloaddition reaction. As a consequence, 110 °C was found to be more suitable for the cycloaddition reaction over the Acen-H catalyst.

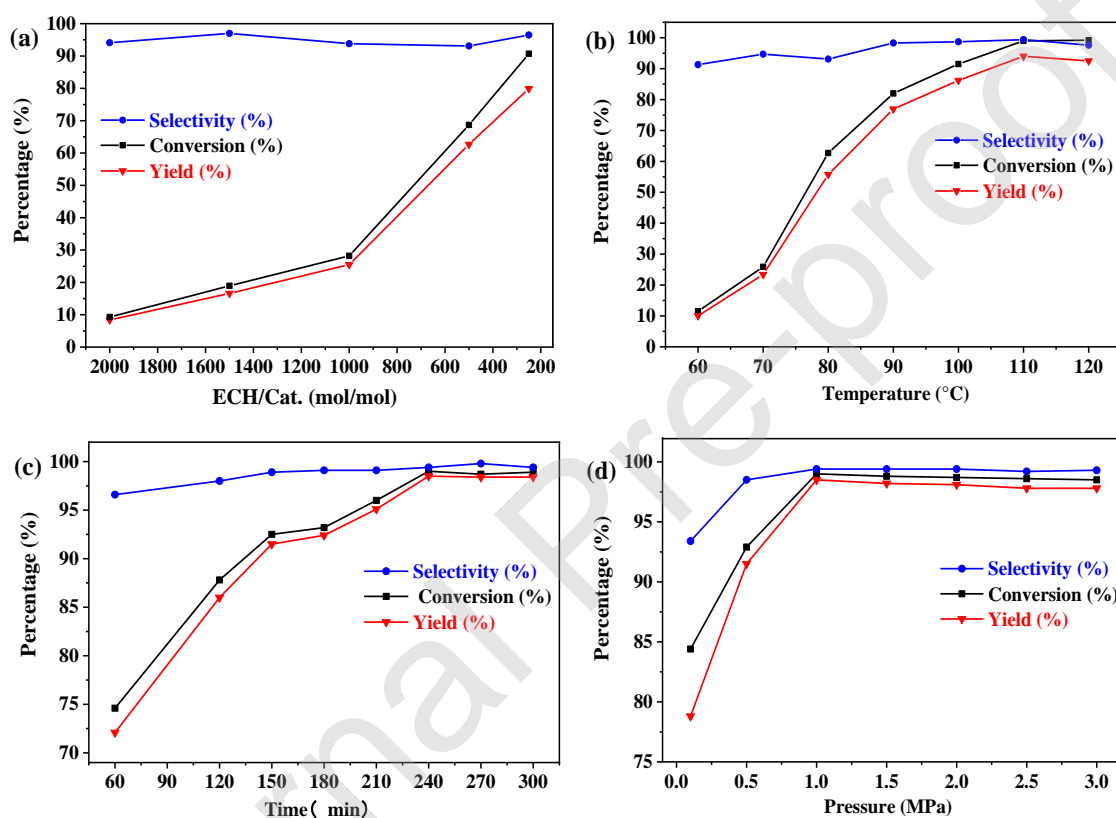
The reaction time was further examined using the above ECH to Acen-H catalyst ratio at 110 °C as shown in Fig. 6(c). When the reaction time was increased from 60 minutes to 240 minutes, the corresponding ECH conversion was increased from 74.6% to 99.0%, the yield increased from 72.1% to 98.5%, and the selectivity increased from 96.6% to 99.4% respectively. This indicates that the duration of reaction has a positive effect on the cycloaddition, and the optimal reaction time was 240 min. Under the above optimized reaction parameters, the effect of initial CO<sub>2</sub> pressure on catalytic performance was investigated as shown in Fig. 6(d). When the CO<sub>2</sub> pressure increased from 0.1 MPa to 1.0 MPa, the reaction showed a positive effect, and a maximum conversion of 99.0%, a yield of 98.5%, and a selectivity of 99.4% was obtained at 1.0 MPa. As the CO<sub>2</sub> pressure



increases, the reaction had a negative effect. Similar results were previously reported for other catalysts [2, 47, 67]. It might be due to difference in the concentration gradient of the reactants in contact with the catalyst at high CO<sub>2</sub> pressures [2]. There are three phase states in the catalytic system, i.e. the upper CO<sub>2</sub> enriched gas phase, the catalyst enriched phase, and the lower ECH enriched liquid phase. The catalytic reaction is expected to be mainly carrying out at the ECH-catalyst interface, and there will be a competitive relationship between these three phases. As the initial CO<sub>2</sub> pressure increases upto an optimal level, the CO<sub>2</sub> concentration in the liquid phase of ECH increases and results in a significant increase in the yield of 3-chloropropylene carbonate. However, when the initial CO<sub>2</sub> pressure far exceeds, the conversion of ECH decreases, and the yield of 3-chloropropylene carbonate also decreases. This might be attributed to the fact that the high CO<sub>2</sub> pressure makes the liquid-phase ECH around the catalyst could be more diluted by the gas-phase CO<sub>2</sub>, so that the liquid-phase ECH cannot fully contact with the catalyst. Due to this, the ECH would not be fully activated by the catalyst and is not conducive to participate in the cycloaddition reaction [2, 47, 67].

In order to verify the catalytic performance of the Acen-H catalyst, its activity was compared with some of the previously reported Schiff base catalysts and the results are summarized in Table 2. Most of the reported catalysts were found to be focused on metal complexes (Table 2, entry 1-8) and used halides (Table 2, entry 1-6, 9) and the catalytic reactions were carried out in solvents (Table 2, entry 1-2). Although the aforesaid catalysts showed good catalytic activity, some of these metal-based catalysts showed low product yield and selectivity in the reaction. Additionally, the metal-based catalysts are toxic in nature and are more susceptible to oxidation, sensitive to hydrolysis, and they would be easily degraded and inactivated in the reaction. Additionally, the use of metal-based catalysts could lead to the leaching of metal ions in the reaction mixture and the contamination of the products, while the use of halides or co-catalysts causes the corrosion of the equipments [26-28]. This is not in line with the concept of green chemistry and economic benefits. In 2019, Wu et al. [26] reported a homogeneous Salophen-H ligand called N,N'-Phenylenebis(5-tert-butylsalicylideneimine) for this reaction. Under meta-, halide- and solvent-free reaction condition, the conversion of ECH and the product yield reached to 84% and 76%, respectively (Table 2, entry 10), at a reaction temperature of 120 °C, a CO<sub>2</sub> pressure of 1.0 MPa for a period of 210 minutes. Our Acen-H catalyst also exhibited high efficiency in the absence of metals, co-catalysts and

solvents at 110 °C, a CO<sub>2</sub> pressure of 1.0 MPa for a reaction time of 210 minutes. The conversion was found to be 96.0% and the yield was 95.1%. When the reaction time was increased to 240 minutes, the conversion and yield reached to 99.0% and 98.5%, respectively (Table 2, entry 11). Therefore, it can be concluded that our Acen-H catalyst shows significant and comparable activity with metal-based catalysts and can be utilized in the absence of co-catalysts or halides and solvents under mild reaction conditions. It validates the potential of Acen-H catalyst for the chemical fixation of CO<sub>2</sub> into cyclic carbonates.



**Fig. 6.** Effect of reaction parameters for CO<sub>2</sub> cycloaddition reaction: (a) effect of ECH/catalyst molar ratio [Acen-H catalyst: 0.1 mmol, epichlorohydrin (ECH): 20-200 mmol, reaction time 240 min, temperature: 80 °C, initial CO<sub>2</sub> pressure: 1 MPa], (b) effect of reaction temperature [Acen-H catalyst: 0.1 mmol, ECH: 50 mmol, reaction time 240 min, initial CO<sub>2</sub> pressure: 1 MPa], (c) effect of reaction time [Acen-H catalyst: 0.1 mmol, ECH: 50 mmol, temperature: 110 °C, initial CO<sub>2</sub> pressure: 1 MPa], (d) effect of initial CO<sub>2</sub> pressure [Acen-H catalyst: 0.1 mmol, ECH: 50 mmol, reaction time 240 min, temperature: 110 °C].

**Table 2.** A comparison of the activity of Schiff base systems for the catalytic ring-opening addition of CO<sub>2</sub> with ECH under different reaction condition.

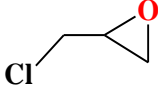
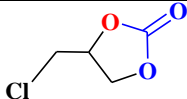
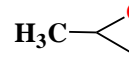
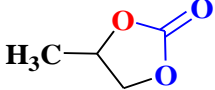

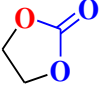
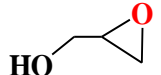
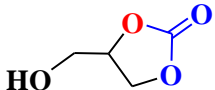
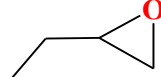
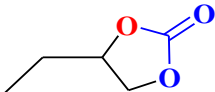
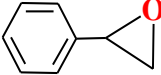
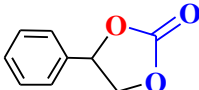
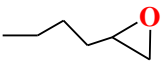
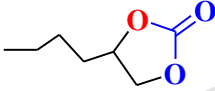
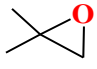
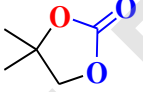
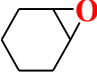
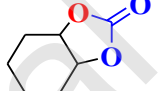
Entry	Catalyst/ Co-Cat./ Solvent	Reaction conditions	Conv. (%)	Yield (%)	TON	TOF	Ref.
1	V <sup>IV</sup> (O)salen (0.01 mol)/ TBAI (0.01 mol)/ MEK (5.0 mL)	45 °C, 1.0 MPa, 18 h	n.d.	96	n.d.	n.d.	[68]
2	Zn(OH-salC <sub>2</sub> NH <sub>2</sub> Am)(0.3 mol%)/ TBAB (10 mg)/ DMF (1.0 mL)	100 °C, 0.1 MPa, 16 h	n.d.	96	n.d.	n.d.	[40]
3	[PS-Zn(II)L] (0.028 mmol)/ TBAB(0.083 mmol)	RT, 0.1 MPa, 8 h	100	≥99	n.d.	n.d.	[24]
4	Zn(salphen)-OCH <sub>3</sub> (0.1 mmol)/ N-methylhomo-piperazine	100 °C, 2.0 MPa, 4 h	n.d.	99	n.d.	n.d.	[25]
5	Zn-CMP(0.1 mol %)/ TBAB (3.6 mol%)	120 °C, 3 MPa, 1 h	n.d.	96.4	n.d.	n.d.	[69]
6	Bimetallic Al(acen) (2.5 mol%)/ TBAB (2.5 mol%)	26 °C, 1.0 atm, 24 h	100	n.d.	n.d.	n.d.	[45]
7	Mono-metallic Al(salen) (0.03 mmol)-ISA-1	100 °C, 1.0 MPa, 0.75 h	97(74)	90(68)	n.d.	240 (181)	[70]
8	Co-Salen-TBB-Py (0.05 g)	80 °C, 0.5 MPa, 8 h	100	n.d.	n.d.	n.d.	[44]
9	Cellulose-based salen complex (Cell-H <sub>2</sub> L)(0.57 mmol)/ TBAB(0.28 mmol)	100 °C, 3.0 MPa, 6 h	99	>99	n.d.	n.d.	[71]
10	N,N'-Phenylenebis(5-tert-butylsalicylideneimine) (1 mol%)	120 °C, 1.0 MPa, 3.5 h	84	76	n.d.	n.d.	[26]
11	N,N'-diphenylene bis(2-hydroxydiene deneimine) (VII) (0.1 mmol)	110 °C, 1.0 MPa, 4 h	99.0	98.5	495.2	123.8	This work

Substrate: epichlorohydrin (ECH); TBAI: Tetrabutylammonium iodide; TBAB: Tetrabutylammonium bromide; MEK: 2-butanone; DMF: N, N-Dimethylformamide; CMP: conjugated microporous polymers; [PS-Zn(II)L]: Zinc chloride coordinated polystyrene supported Schiff base ligand [PS-H<sub>2</sub>L]; n.d. : Means not reported in the literature.

Based on the above optimized reaction conditions, the catalytic performance of the Acen-H catalyst was further investigated for the cycloaddition of different epoxides with CO<sub>2</sub>, and the

corresponding results are summarized in Table 3. The experimental data shows that among the nine epoxides tested, the Acen-H catalyst shows better catalytic activity for four of them than the other epoxides (Table 3, entry 1-4). Compared with other epoxides, epichlorohydrin (ECH) achieved the highest yield in 4.0 h (Table 3, entry 1). Obviously, the activity of ECH was superior to other epoxides. It could be related to the substitution of halide group at the end of epoxide. During the reaction, the activation of ECH molecule produces some chloride anions ( $\text{Cl}^-$ ). These chloride anions can act as a nucleophile to attack the  $\text{C}_\beta$  position of the epoxide to promote its ring opening and forms an intermediate compound containing chloride anions, which can also assist in the ring opening of other epoxide molecules in the reaction mixture [47, 72]. In addition, the chloride of ECH can act as an electron withdrawing group, thereby reducing the electron cloud density of the C-O bond of ECH, which further promotes its ring-opening. However, due to the structural symmetry of ethylene oxide and its uniform electron cloud density around the two C-O bondings and also due to the absence of any end groups, the probability of the activation of two C-O bonds of ethylene oxide is high, when it is came in contact with the catalyst [73, 74]. That is, the C-O bond of ethylene oxide is relatively easy to break in the ring-opening stage of the process compared to other epoxides, which enhances its cycloaddition reaction. Therefore, the conversion of ethylene oxide is relatively high (Table 3, entry 3). However, as for cyclohexane oxide, no conversion was obtained for a period of 30 h of reaction, indicating the incapability of the Acen-H catalyst for cyclohexane oxide conversion. It could be due to the inner-ring structural effects as well as its high steric hindrance [75, 76]. Moreover, it requires a higher activation energy to overcome the steric hindrance to activate the ring opening (Table 3, entry 10). According to the significant variations in the activity of the prepared catalyst for different epoxides, it can be said that the Acen-H catalyst catalyzes the cycloaddition of  $\text{CO}_2$  with terminal epoxides containing a halide or electron-withdrawing groups as reactants, while with the inner epoxides, it shows very low catalytic activity at the same experimental conditions. Therefore, Acen-H catalyst is more suitable for catalyzing the reaction with terminal epoxides containing halide or electron-withdrawing groups as reactants.

**Table 3.** Performance of the Acen-H catalyst for the ring-opening addition of  $\text{CO}_2$  with different epoxides

Entry <sup>[a]</sup>	Substrate	Product	Time (h)	Conv. (%) <sup>[b]</sup>	Yield (%)	Select. (%)	TON <sup>[c]</sup>
1			4.0	99.0	98.5	99.4	495.2
2			3.5	47.6	40.9	86.0	238.0
			6.0	94.6	94.4	99.7	473.2
3			4.0	91.1	89.5	98.3	455.5
			6.0	99.6	96.3	96.6	498.0
4			4.0	77.9	76.1	97.7	389.5
5			3.5	42.7	42.5	99.7	213.4
			10.0	54.4	54.2	99.7	457.4
6			12.0	56.6	56.4	99.6	283.2
7			4.0	0	0	0	0
			16.0	40.4	40.1	99.2	202.2
8			4.0	12.8	11.9	93.0	63.9
			10.0	34.3	32.2	94.0	171.3
9			20.0	0	0	0	0
			30.0	0	0	0	0

[a] Reaction Conditions: Acen-H catalyst (VII) (0.1 mmol), substrate (50 mmol), temperature 110 °C, CO<sub>2</sub> pressure 1 MPa, 280 rpm magnetic stirring rate, [b] Determined by <sup>1</sup>H-NMR spectroscopy using TMS as an internal standard, [c] TON (Turnover number) = molar amount of initial substrate \* conversion / molar amount of catalyst.

### 3.3. Reaction kinetics and mechanism

The reaction kinetics for the cycloaddition of CO<sub>2</sub> with ECH catalyzed by Acen-H catalyst was further studied. The rate equation for the cycloaddition reaction was expressed as follows:

$$\text{Rate} = k [\text{ECH}]^a [\text{CAT}]^b [\text{CO}_2]^c$$

in which '*k*' denotes the rate constant, [ECH], [CAT] and [CO<sub>2</sub>] represents the concentrations of epoxide, Acen-H catalyst and CO<sub>2</sub> respectively, whereas *a*, *b* and *c* denote the orders of the

corresponding reactants. Based on the assumption that the formation of cyclic carbonates follows first order kinetics with respect to CO<sub>2</sub> [37, 77] and the concentration of Acen-H catalyst did not change during the reaction, the above equation can also be written as follows [77]:

$$\text{Rate} = k_{\text{obs}}[\text{ECH}]^a, \text{ where } k_{\text{obs}} = k[\text{CAT}]^b[\text{CO}_2]$$

$$\text{Rate} = -d[\text{ECH}]/dt = k_{\text{obs}}[\text{ECH}]$$

where  $k_{\text{obs}}$  represents the pseudo-first order rate constant for the conversion of ECH [78].

By the integration of above equations, the following expression can be obtained.

$$-\ln[\text{ECH}] = k_{\text{obs}}t$$

Additionally, to understand the reaction kinetics in the synthesis of cyclic carbonates from CO<sub>2</sub> and epoxides, the parameters were further investigated at different reaction temperatures of 80 °C, 90 °C, 100 °C and 110 °C. The concentration of ECH with reaction time for the ring-opening at different reaction temperatures is shown in Fig. 7(a). According to the above formula, the  $-\ln[\text{ECH}]$  was found to be linearly fitted with reaction time. The slope of the fitted line followed pseudo-first-order kinetics with the rate constant of  $k$  at different temperatures. The resulted fitting plots are shown in Fig. 7(b).

The rate equation, correlation coefficient  $R^2$ , reaction rate constant  $k_{\text{obs}}$  and natural logarithm of  $\ln k_{\text{obs}}$  at different temperatures are listed in the Table 4. It is concluded that the correlation coefficients  $R^2$  was found to be close to 1, which indicates that the reaction rate is linear with the concentration of ECH and follows pseudo first-order kinetic reaction [52, 77]. Arrhenius equation was further adopted to calculate the activation energy [52]. The observed rate constant is given by the expression:

$$k_{\text{obs}} = A \exp(-E_a/RT)$$

In this formula,  $A$ : pre-exponential factor ( $\text{min}^{-1}$ );  $T$ : absolute temperature (K);  $E_a$ : apparent activation energy (kJ/mol);  $R$ : ideal gas constant ( $8.314 \text{ J}\cdot\text{mol}^{-1}\text{K}^{-1}$ ).

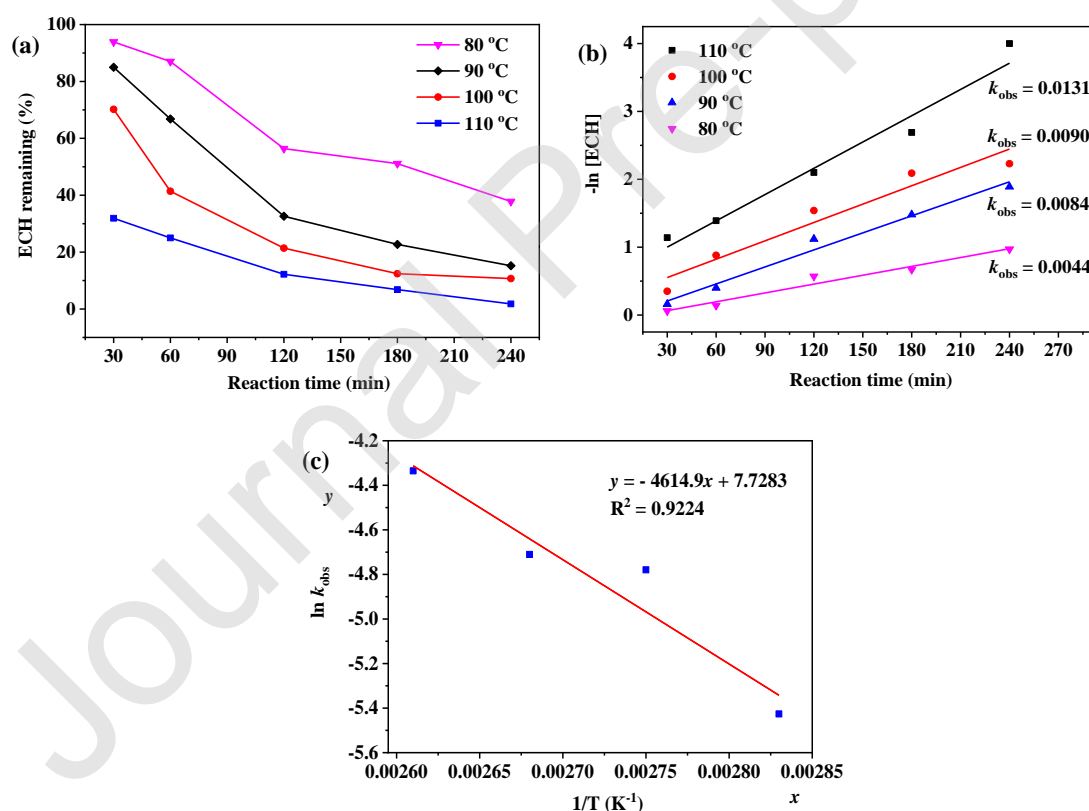
$$\ln k_{\text{obs}} = \ln A - E_a/RT$$

In the temperature range of 80-110 °C, the data was linearly fitted by  $\ln k$  with  $1/T$  ( $\text{K}^{-1}$ ), and the fitting equation is given by the expression  $y = -4614.9x + 7.7283$  (Fig. 7(c)). It was concluded that the pre-exponential factor and apparent activation energy for the Acen-H catalyst catalyzed ring-opening addition of CO<sub>2</sub> with ECH were found to be  $A = 2.272 \times 10^3 \text{ min}^{-1}$  and  $E_a = 38.368 \text{ kJ}\cdot\text{mol}^{-1}$ , respectively.

The rate equation can be thus written as:

$$\text{Rate} = -d[\text{ECH}]/dt = 2.272 \times 10^3 [\text{ECH}] \exp(-38.368/(RT)).$$

The activation energy required for the cycloaddition of CO<sub>2</sub> with ECH was previously reported over a series of catalyst systems. For example, Briana et al. [79] reported an activation energy of 63.6 kJ·mol<sup>-1</sup> for the aforesaid cycloaddition reaction over a MIL-101-IP MOF catalyst at 298K and 313K. Wu et al. [80] reported an activation energy of 113.38 kJ·mol<sup>-1</sup> over a Zn-BTC-2MeIm MOF catalyst for the reaction, performed at 363K-373K. In other work, Samanta et al. [81] reported a bifunctional graphitic carbon nitride S-CN(UTU)-60 catalyst for the cycloaddition reaction at 333K-383K, with an activation energy of 55.33 kJ·mol<sup>-1</sup>. Wu et al. [82] reported an activation energy of 98.5 kJ·mol<sup>-1</sup> for the reaction over a bifunctional (salen)cobalt(III)-based catalyst. Thus, it is clear that the activation energy for cycloaddition reaction catalyzed the Acen-H catalyst is quite small compared to the previously reported metal based catalysts.

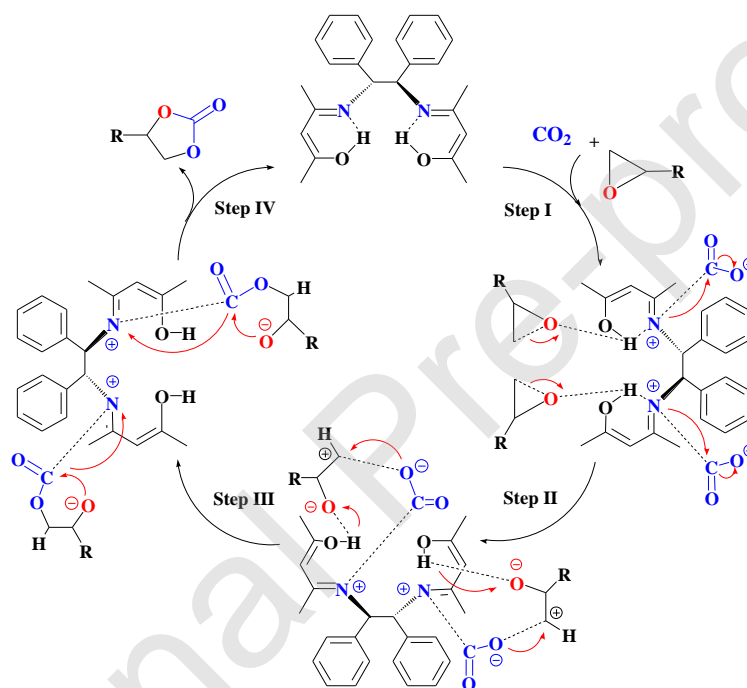


**Fig. 7.** The cycloaddition of CO<sub>2</sub> catalyzed by Acen-H catalyst at different reaction temperatures: (a) the curve of ECH residual concentration versus reaction time; (b)  $-\ln[\text{ECH}]$  linear fitting relationship with reaction time; (c) Arrhenius equation linear fitting to obtain activation

energy and the pre-exponential factor. Reaction conditions: Acen-H catalyst (0.05 mmol), ECH (25 mmol), Pressure (CO<sub>2</sub>) = 1 MPa.

**Table 4.** Reaction kinetics equation and kinetic parameters at different reaction temperatures

T(°C)	Kinetic equation	R <sup>2</sup>	1/T(K <sup>-1</sup> )	k <sub>obs</sub> (min <sup>-1</sup> )	ln k <sub>obs</sub>
110	y = 0.0131x + 0.6101	0.9585	0.0026	0.0131	-4.3351
100	y = 0.0090x + 0.2820	0.9186	0.0027	0.0090	-4.7105
90	y = 0.0084x - 0.0438	0.9766	0.0028	0.0084	-4.7795
80	y = 0.0044x - 0.0658	0.9576	0.0028	0.0044	-5.4261



**Fig. 8.** Plausible mechanism for the ring-opening addition reaction of CO<sub>2</sub> with epoxide to synthesize cyclic carbonate over Acen-H catalyst.

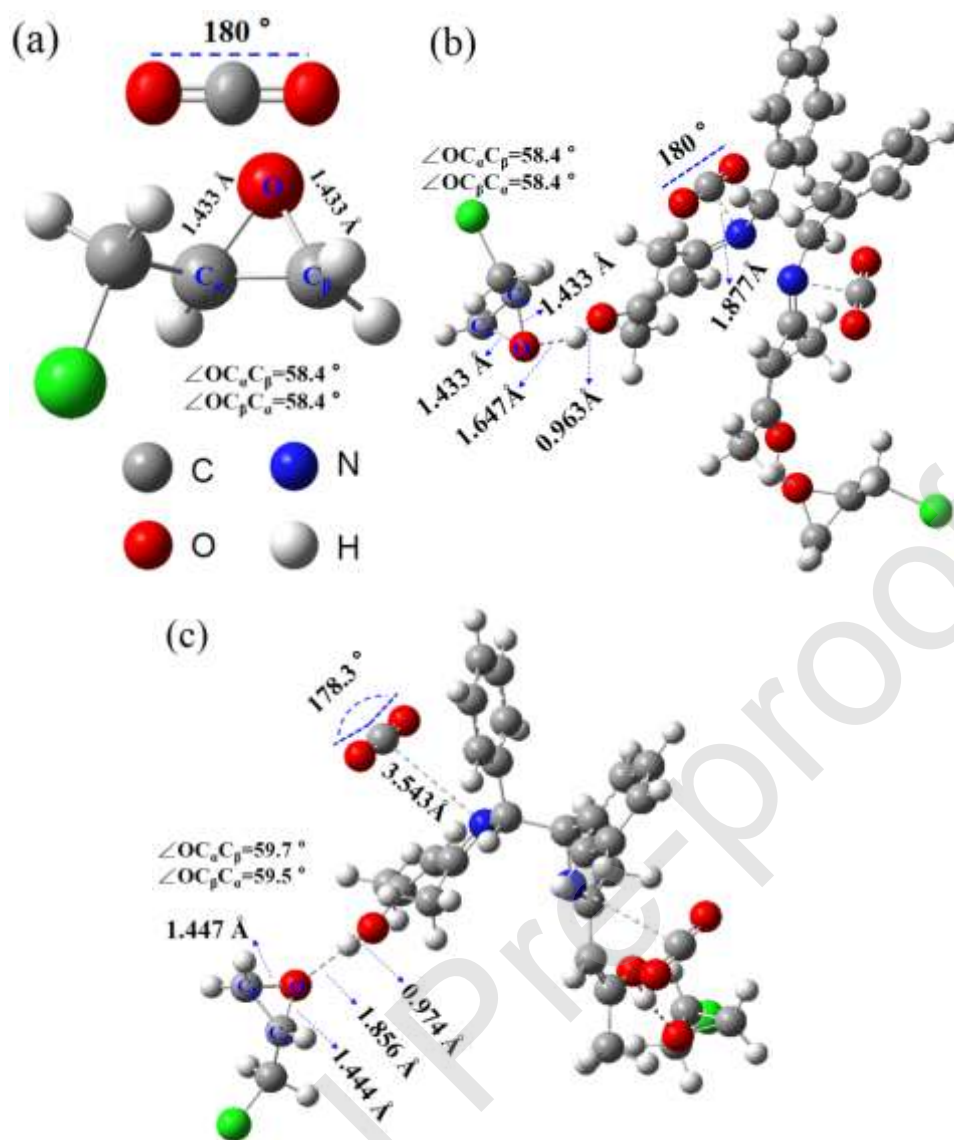
A reasonable reaction mechanism is proposed for the catalytic activity. As shown in Fig. 8, the imino group (-N=) on the Acen-H catalyst provides Lewis basic sites for the adsorption and activation of CO<sub>2</sub> molecule [77, 83]. The -OH group in the Acen-H catalyst acts as a hydrogen bond donor, which facilitates the epoxide activation by attacking the oxygen in epoxide and forming a hydrogen bond [40, 84]. The hydrogen bond formation is critical in the epoxide activation. It polarizes the carbon-oxygen bond in the epoxide and weakens their electron cloud density. Among them, the C<sub>β</sub>-O bond with less steric hindrance and low extranuclear electron cloud density can be



---

easily opened by the hydrogen bond and an activated intermediate complex would be formed [42, 85]. Thereafter, the oxyanion in the activated CO<sub>2</sub> attacks the C<sub>β</sub> position of the epoxide (C<sub>β</sub><sup>+</sup>) and a new C-O bond would be formed, which further results in the formation of a carbonic half-ester intermediate [26]. Moreover, the additional hydrogen-bond (=N---H) formed in between the imino group (-N=) and H of the hydroxyl group has a synergistic effect in the polarization of C-O bond in the epoxide [40, 85]. The formed carbonic half-ester intermediate further undergoes a intramolecular nucleophilic attack followed by an electron transfer [83]. The oxyanion of the epoxide moiety in the carbonic half ester intermediate further attacks the C atom of the CO<sub>2</sub> and the loop gets closed [86]. As a result, the effects of hydrogen bonding could be weakened and the formed cyclic carbonate can be desorbed.

The experimental and mechanistic studies of the cycloaddition of CO<sub>2</sub> with epoxides show that the ring-opening of epoxide is considered as a rate control step in the cycloaddition of carbon dioxide [10]. In addition, because of the high first ionization energy (13.97 eV) and high electron affinity (38 eV) of CO<sub>2</sub>, it acts as a weak electron donor and a strong electron acceptor, while the epoxide acts as an electron donor [87]. Therefore, the interaction of CO<sub>2</sub> and epoxides can effectively enhance the solubility of CO<sub>2</sub> in the reaction medium [70].



**Fig. 9.** DFT studies on the intermolecular interaction of the Acen-H catalyst with CO<sub>2</sub> and epichlorohydrin: (a) CO<sub>2</sub> and epichlorohydrin, (b) before optimization, (c) after optimization.

In order to validate the reaction mechanism, DFT calculations were performed using Gaussian 09 program with standard B3LYP/6-311+G (d, p) basis set. The interactions of the equilibrium geometry of Acen-H catalyst with epichlorohydrin and CO<sub>2</sub> were considered from the geometric optimizations method [42, 43] and the obtained results are shown in Fig. 9. The results had shown that the C<sub>α</sub>-O bond in ECH increased from 1.433 Å to 1.444 Å, while the C<sub>β</sub>-O bond increased from 1.433 Å to 1.447 Å, and ∠OC<sub>α</sub>C<sub>β</sub> and ∠OC<sub>β</sub>C<sub>α</sub> bond angles changed from 58.4° to 59.7° and 59.5° respectively. This indicates that the hydrogen bond polarizes the C-O bond of ECH and promotes its breaking and ring-opening. Among them, C<sub>β</sub>-O bond was easier to open. The hydrogen bond also increased from 1.647 Å to 1.856 Å, indicating the existence of a polarized complex desorption

process. The O-H bond of the hydroxyl functional group in the Acen-H catalyst also increased from 0.963 Å to 0.974 Å during polarization. In addition, the linear CO<sub>2</sub> molecule was changed to a 178.3° curved structure from its 180° geometry. Moreover, the C-N bond was increased to 3.543 Å from 1.877 Å. This indicates that there is a desorption process from the imino group and these calculations further validated the proposed reaction mechanism.

#### 4. Conclusions

Compared to the commonly reported metal-based Schiff base catalysts containing a metal ion to provide Lewis active sites, a metal-free Acen-H catalyst was successfully synthesized and used as an excellent homogenous catalyst in the cycloaddition of CO<sub>2</sub> with epichlorohydrin (ECH) to produce corresponding cyclic carbonates. A high epoxide conversion and cyclic carbonate selectivity and yield were achieved for several epoxides like epichlorohydrin, propylene oxide and ethylene oxide over the prepared Acen-H catalyst. The optimization of reaction parameters indicated that a maximum epoxide conversion of 99.0% with 99.4% selectivity and 98.5% yield was obtained at a reaction temperature of 110 °C, an initial CO<sub>2</sub> pressure of 1.0 MPa and an epoxide to catalyst ratio of 500 for a period of 240 minutes of reaction. The Acen-H catalyst exhibited higher catalytic activity compared to the Salophen-H ligands due to the negative effect of delocalized  $\pi$  electrons in the Salophen-H ligands. The catalytic activity of the Acen-H catalyst is derived from the active hydrogen bond donors (-O-H, =N---H) and imino groups (-N=), which played a synergistic role in the adsorption and activation of reactant molecules. These characteristics of functional groups in the catalyst structure can effectively replace the metal ions and halides for the activation and ring opening of epoxides. Here, the importance of the structural characteristics of Acen-H catalyst for the cycloaddition reaction is further illustrated.

#### **Credit authorship contribution statement:**

**Z. Yue:** Conceptualization, Investigation, Methodology, Formal analysis, Data curation, Writing – Original draft preparation.

**M. Pudukudy:** Writing – review & editing, Supervision, Funding acquisition.

**S. Chen:** Writing – review & editing.

**Y. Liu:** Writing – review & editing.

**W. Zhao:** Writing – review & editing.

**J. Wang:** Writing – review & editing.

**S. Shan:** Resources, Writing – review & editing, Supervision, Funding acquisition, Project administration.

**Q. Jia:** Resources, Writing – review & editing.

### **Declaration of Interest Statement:**

There are no conflicts of interests to declare.

### **Conflicts of Interest**

There are no conflicts of interests to declare.

### **Acknowledgements**

This study was financially supported by the National Natural Science Foundation of China (Grant No. 21766016), the Yunnan Ten Thousand Talents Plan Young & Elite Talents Project (YNWR-QNBJ-2018-198), the Academician Workstation (2019IC002), the Talent Reserve Project in Yunnan (2015HB014), the Kunming Science and Technology Planning Project (2019-1-G-25318000003480), and the China Postdoctoral Science Foundation (Grant No. 2019M653845XB).

### **References**

- [1] J. A. James, S. Sung, H. Jeong, O. A. Broesicke, S. P. French, D. Li, J. C. Crittenden, *Environ. Sci. Technol.* 52 (2018) 3-10. <https://doi.org/10.1021/acs.est.7b01115>
- [2] J. Peng, S. Wang, H.-J. Yang, B. Ban, Z. Wei, L. Wang, B. Lei, *Fuel* 224 (2018) 481-488. <https://doi.org/10.1016/j.fuel.2018.03.119>
- [3] J. Klankermayer, S. Wesselbaum, K. Beydoun, W. Leitner, *Angew. Chem. Int. Ed.* 47 (2016) 7267-7267. <https://doi.org/10.1002/anie.201507458>
- [4] T. T. Liu, J. Liang, R. Xu, Y. B. Huang, R. Cao, *Chem. Commun.* 55 (2019) 4063-4066. <https://doi.org/10.1039/C8CC10268F>
- [5] P. Puthiaraj, S. Ravi, K. Yu, W.-S. Ahn, *Appl. Catal. B* 251 (2019) 195-205. <https://doi.org/10.1016/j.apcatb.2019.03.076>

- 
- [6] B. Grignard, S. Gennen, C. Jérme, A. W. Kleij, C. Detrembleur, *Chem. Soc. Rev.* 48 (2019) <http://doi.org/10.1039/C9CS00047J>
- [7] A. J. Kamphuis, F. Picchioni, P. P. Pescarmona, *Green Chem.* 21 (2019) 406-448. <http://doi.org/10.1039/c8gc03086c>
- [8] K. Tomishige, H. Yasuda, Y. Yoshida, M. Nurunnabi, B. Li, K. Kunimori, *Green Chem.* 6 (2004) 206-214. <https://doi.org/10.1039/B401215A>
- [9] J. Ma, J. Liu, Z. Zhang, B. Han, *Comput. Theor. Chem.* 992 (2012) 103-109. <https://doi.org/10.1016/j.comptc.2012.05.010>
- [10] Y. Chen, R. Luo, Q. Xu, W. Zhang, X. Zhou, H. Ji, *Chemcatchem* 9 (2017) 767-773. <https://doi.org/10.1002/cctc.201601578>
- [11] T. Schwander, v. B. L. Schada, S. Burgener, N. S. Cortina, T. J. Erb, *Science* 354 (2016) 900-904. <https://doi.org/10.1126/science.aah5237>
- [12] J. W. Comerford, I. D. V. Ingram, M. North, X. Wu, *Green Chem.* 46 (2015) 1966-1987. <https://doi.org/10.1039/C4GC01719F>
- [13] B. Schaffner, F. Schaffner, S. P. Verevkin, A. Borner, *Chem. Rev.* 110 (2010) 4554-4581. <https://doi.org/10.1021/cr900393d>
- [14] A. A. Chaugule, A. H. Tamboli, H. Kim, *Fuel* 200 (2017) 316-332. <http://doi.org/10.1016/j.fuel.2017.03.077>
- [15] Q.-W. Song, L.-N. He, J.-Q. Wang, H. Yasuda, T. Sakakura, *Green Chem.* 15 (2013) 110-115. <https://doi.org/10.1039/C2GC36210D>
- [16] X. B. Lu, *Top. Organometal. Chem.* 53 (2015) 171-198. [https://doi.org/10.1007/3418\\_2015\\_98](https://doi.org/10.1007/3418_2015_98)
- [17] M. Fleischer, H. Blattmann, R. Mülhaupt, *Green Chem.* 15 (2013) 934-942. <https://doi.org/10.1039/C3GC00078H>
- [18] M. Bähr, R. Mülhaupt, *Green Chem.* 14 (2012) 483-489. <https://doi.org/10.1039/C2GC16230J>
- [19] M. Alves, B. Grignard, R. Mereau, C. Jerome, T. Tassaing, C. Detrembleur, *Catal. Sci. Technol.* 7 (2017) 2651-2684. <https://doi.org/10.1039/C7CY00438A>
- [20] J. L. S. Milani, I. S. Oliveira, P. A. D. Santos, A. K. S. M. Valdo, F. T. Martins, D. Cangussu, R. P. D. Chagas, *Chin. J. Catal.* 39 (2018) 245-249. [https://doi.org/10.1016/S1872-2067\(17\)62992-9](https://doi.org/10.1016/S1872-2067(17)62992-9)
- [21] Q. Han, B. Qi, W. Ren, C. He, J. Niu, C. Duan, *Nat. Commun.* 6 (2015) 10007. <https://doi.org/10.1038/ncomms10007>

- [22] T. Ema, Y. Miyazaki, J. Shimonishi, C. Maeda, J. Y. Hasegawa, *J. Am. Chem. Soc.* 136 (2016) 15270-15279. <https://doi.org/10.1021/ja507665a>
- [23] M. B. Gawande, R. K. Pandey, R. V. Jayaram, *Cheminform* 43 (2012) 1113-1125. <https://doi.org/10.1002/chin.201234214>
- [24] S. Biswas, R. Khatun, M. Sengupta, S. M. Islam, *Mol. Catal.* 452 (2018) 129-137. <https://doi.org/10.1016/j.mcat.2018.04.009>
- [25] Y. Ren, J. Chen, C. Qi, H. Jiang, *Chemcatchem* 7 (2015) 1535-1538. <https://doi.org/10.1002/cctc.201500113>
- [26] X. Wu, C. Chen, Z. Guo, M. North, A. C. Whitwood, *ACS Catalysis* 9 (2019) 1895-1906. <https://doi.org/10.1021/acscatal.8b04387>
- [27] Dong-Hui, Lan, Na, Fan, Ying, Wang, Xian, Gao, Ping, Zhang, *Chinese Journal of Catalysis* (2016) [http://doi.org/10.1016/S1872-2067\(15\)61085-3](http://doi.org/10.1016/S1872-2067(15)61085-3)
- [28] N. Zhang, B. Zou, G. Yang, B. Yu, C. Hu, *Journal of CO<sub>2</sub> Utilization* 22 (2017) 9-14. <http://dx.doi.org/10.1016/j.jcou.2017.09.001>
- [29] C. Baleizao, H. Garcia, *Chem. Rev.* 106 (2006) 3987-4043. <https://doi.org/10.1021/cr050973n>
- [30] A. Coletti, C.J. Whiteoak, D.V. Conte, D.A.W. Kleij, *Chemcatchem* 4 (2012) 1190-1196. <https://doi.org/10.1002/cctc.201100398>
- [31] X. B. Lu, D. J. Darensbourg, *Chem. Soc. Rev.* 41 (2012) 1462-1460. <http://doi.org/10.1039/c1cs15142h>
- [32] Z. Bo, C. Hu, *Curr. Opin. Green Sustain. Chem.* 3 (2017) 11-16. <https://doi.org/10.1016/j.cogsc.2016.10.007>
- [33] C. J. Whiteoak, A. H. Henseler, C. Ayats, A. W. Kleij, M. A. Pericàs, *Green Chem.* 16 (2014) 1552-1559. <https://doi.org/10.1039/C3GC41919C>
- [34] M. Cokoja, M. E. Wilhelm, M. H. Anthofer, W. A. Herrmann, F. E. Kuehn, *Chemsuschem* 46 (2015) 2436-2454. <https://doi.org/10.1002/cssc.201500161>
- [35] J. Sun, L. Han, W. Cheng, J. Wang, X. Zhang, S. Zhang, *Chemsuschem* 4 (2011) 502-507. <https://doi.org/10.1002/cssc.201000305>
- [36] X.-F. Liu, Q.-W. Song, S. Zhang, L.-N. He, *Catal. Today* 263 (2016) 69-74. <https://doi.org/10.1016/j.cattod.2015.08.062>
- [37] M. Liu, L. Liang, X. Li, X. Gao, J. Sun, *Green Chem.* 18 (2016) 2851-2863. <https://doi.org/10.1039/C5GC02605A>

- [38] L. Wang, G. Zhang, K. Kodama, T. Hirose, *Green Chem.* 47 (2016) 1229-1233. <https://doi.org/10.1039/C5GC02697K>
- [39] Y. Kobayashi, R. Obayashi, Y. Watanabe, H. Miyazaki, I. Miyata, Y. Suzuki, Y. Yoshida, T. Shioiri, M. Matsugi, *Eur. J. Org. Chem.* 2019 (2019) 2401-2408. <https://doi.org/10.1002/ejoc.201900146>
- [40] X. D. Lang, Y. C. Yu, L. N. He, *J. Mol. Catal. A: Chem.* 420 (2016) 208-215. <https://doi.org/10.1016/j.molcata.2016.04.018>
- [41] R. Ma, L. N. He, X. F. Liu, X. Liu, M. Y. Wang, *J. CO<sub>2</sub> Util.* 19 (2017) 28-32. <https://doi.org/10.1016/j.jcou.2017.03.002>
- [42] M. Zhang, B. Chu, G. Li, J. Xiao, H. Zhang, Y. Peng, B. Li, P. Xie, M. Fan, L. Dong, *Micropor. Mesopor. Mat.* 274 (2019) 363-372. <https://doi.org/10.1016/j.micromeso.2018.09.011>
- [43] K. R. Roshan, B. M. Kim, A. C. Kathalikkattil, J. Tharun, Y. S. Won, D. W. Park, *Chem. Commun.* 50 (2014) 13664-13667. <https://doi.org/10.1039/C4CC04195J>
- [44] C. Zhang, D. Lu, Y. Leng, P. Jiang, *Mol. Catal.* 439 (2017) 193-199. <https://doi.org/10.1016/j.mcat.2017.07.002>
- [45] M. North, C. Young, *Catal. Sci. Technol.* 1 (2011) 93-99. <https://doi.org/10.1039/C0CY00023J>
- [46] W. H. Woo, K. Hyun, Y. Kim, J. Y. Ryu, J. Lee, M. Kim, M. H. Park, Y. Kim, *Eur. J. Inorg. Chem.* 45 (2017) 5372-5378. <https://doi.org/10.1002/ejic.201701169>
- [47] X. Song, Y. Wu, D. Pan, R. Wei, L. Gao, J. Zhang, G. Xiao, *J. CO<sub>2</sub> Util.* 24 (2018) 287-297. <https://doi.org/10.1016/j.jcou.2018.01.017>
- [48] P. Skrdla, V. Antonucci, C. Lindemann, *J. Chromatogr. Sci.* 39 (2001) 431-440. <https://doi.org/10.1093/chromsci/39.10.431>
- [49] D. T. Mauney, J. A. Maner, M. A. Duncan, *J. Phys. Chem. A* 121 (2017) 7059-7069. <https://doi.org/10.1021/acs.jpca.7b07180>
- [50] K. A. Manbeck, N. C. Boaz, N. C. Bair, A. M. S. Sanders, A. L. Marsh, *J. Chem. Educ.* 88 (2011) 1444-1445. <https://doi.org/10.1021/ed1010932>
- [51] K. J. Davis, C. Richardson, J. L. Beck, B. M. Knowles, A. Guédin, J.-L. Mergny, A. C. Willis, S. F. Ralph, *Dalton T.* 44 (2015) 3136-3150. <https://doi.org/10.1039/C4DT02926G>
- [52] S. Supasitmongkol, P. Styring, *Catal. Sci. Technol.* 4 (2014) 1622-1630. <https://doi.org/10.1039/C3CY01015E>

- [53] G. Morales, X. Delgado, L. Galeano, J. CO<sub>2</sub> Util. 12 (2015) 82-85.  
<https://doi.org/10.1016/j.jcou.2015.06.002>
- [54] M. Shakir, N. Begum, S. Parveen, P. Chingsubam, S. Tabassum, Synth. React. Inorg. Met.-Org. Chem. 34 (2004) 1135-1148. <https://doi.org/10.1081/SIM-120039262>
- [55] T. J. Zielinski, A. Grushow, J. Chem. Educ. 79 (2002) 707-714. <https://doi.org/10.1021/ed079p707>
- [56] F. Firdaus, J. Coord. Chem. 63 (2010) 3956-3968. <https://doi.org/10.1080/00958972.2010.526707>
- [57] C. Sutton, N. R. Tummala, T. Kemper, S. G. Aziz, J. Sears, V. Coropceanu, J.-L. Brédas, J. Chem. Phys. 146 (2017) 1-5. <https://doi.org/10.1063/1.4984783>
- [58] T. M. Krygowski, B. T. Stępień, Chem. Rev. 105 (2005) 3482-3512. <https://doi.org/10.1021/cr030081s>
- [59] H. Szatyłowicz, A. Jezuita, K. Ejsmont, T. M. Krygowski, J. Mol. Model. 25 (2019) 1-7.  
<https://doi.org/10.1007/s00894-019-4204-3>
- [60] X. B. Lu, D. J. Darensbourg, Chem. Soc. Rev. 41 (2012) 1462-1484. <http://doi.org/10.1039/c1cs15142h>
- [61] T. P. A. Cao, G. Nocton, L. Ricard, X. F. Le. Goff, A. Auffrant, Angew. Chem. 126 (2014) 1392-1396.  
<http://doi.org/10.1002/ange.201309222>
- [62] E. Carter, I. A. Fallis, B. M. Kariuki, I. R. Morgan, D. M. Murphy, T. Tatchell, S. Van Doorslaer, E. Vinck, Dalton Transactions 40 (2011) 7454. <http://doi.org/10.1039/c1dt10378d>
- [63] Y. Niu, H. Li, Colloid & Polymer Science 291 (2013) 2181-2189. <http://doi.org/10.1007/s00396-013-2957-2>
- [64] V. Delchev, J. Struct. Chem. 44 (2003) 574-580. <https://doi.org/10.1023/B:JORY.0000017932.70437.40>
- [65] M. N. Sheng, J. Heterocycl. Chem. 6 (2009) 651-654. <http://doi.org/10.1002/jhet.5570060510>
- [66] B. L. Fitzpatrick, B. W. Alligood, L. J. Butler, S. H. Lee, J. M. Lin, J. Chem. Phys. 133 (2010) 094306.  
<http://dx.doi.org/10.1063/1.3475001>
- [67] J. Sun, J. Wang, W. Cheng, J. Zhang, X. Li, S. Zhang, Y. She, Green Chemistry 14 (2012) 654-660.  
<https://doi.org/10.1039/C2GC16335G>
- [68] A. Coletti, C. J. Whiteoak, V. Conte, A. W. Kleij, ChemCatChem 4 (2012) 1190-1196.  
<https://doi.org/10.1002/cctc.201100398>
- [69] Y. Xie, T. T. Wang, R. X. Yang, N. Y. Huang, K. Zou, W. Q. Deng, Chemsuschem 7 (2014) 2110-2114.  
<https://doi.org/10.1002/cssc.201402162>
- [70] R. Luo, X. Zhou, S. Chen, Y. Li, L. Zhou, H. Ji, Green Chem. 16 (2014) 1496-1506.  
<https://doi.org/10.1039/C3GC42388C>



- [71] S. Chen, M. Pudukudy, Z. Yue, H. Zhang, Y. Zhi, Y. Ni, S. Shan, Q. Jia, *Ind. Eng. Chem. Res.* 58 (2019) 17255-17265. <https://doi.org/10.1021/acs.iecr.9b03331>
- [72] X. Song, Y. Wu, D. Pan, F. Cai, G. Xiao, *Mol. Catal.* 436 (2017) 228-236. <https://doi.org/10.1016/j.mcat.2017.04.027>
- [73] R. Hemmati, K. Patkowski, *The Journal of Physical Chemistry A* (2019) <http://doi.org/10.1021/acs.jpca.9b06028>
- [74] M. North, P. Villuendas, C. Young, *Chemistry* 15 (2009) 11454-11457. <http://doi.org/10.1002/chem.200902436>
- [75] Y. Jiang, J. Li, P. Jiang, Y. Li, Y. Leng, *Catal. Commun.* 111 (2018) 1-5. <https://doi.org/10.1016/j.catcom.2018.03.030>
- [76] T. Werner, N. Tenhumberg, *J. CO<sub>2</sub> Util.* 7 (2014) 39-45. <https://doi.org/10.1016/j.jcou.2014.04.002>
- [77] B. Zou, L. Hao, L.-Y. Fan, Z.-M. Gao, S.-L. Chen, H. Li, C.-W. Hu, *J. Catal.* 329 (2015) 119-129. <https://doi.org/10.1016/j.jcat.2015.05.002>
- [78] M. Liu, L. Bo, S. Zhong, S. Lei, J. Sun, *Ind. Eng. Chem. Res.* 54 (2015) 633-640. <https://doi.org/10.1021/ie5042879>
- [79] A. Briana, S. Qi, X. Wang, O. R. Erica, A. M. Al-Enizi, N. Ayman, S. Ma, *Angew. Chem. Int. Ed.* (2018) <http://doi.org/10.1002/anie.201803081>
- [80] Y. Wu, X. Song, J. Zhang, S. Xu, N. Xu, H. Yang, Y. Miao, L. Gao, J. Zhang, G. Xiao, *Chemical Engineering Research & Design* (2018) <http://doi.org/10.1016/j.cherd.2018.10.034>
- [81] S. Samanta, R. Srivastava, *Sustainable Energy Fuels* (2017) 10.1039/C7SE00223H. <http://doi.org/10.1039/C7SE00223H>
- [82] G. P. Wu, S. H. Wei, W. M. Ren, X. B. Lu, T. Q. Xu, D. J. Darensbourg, *J. Am. Chem. Soc.* 133 (2011) p.15191-15199. <http://dx.doi.org/10.1021/ja206425j>
- [83] A. Samikannu, L. J. Konwar, P. Mäki-Arvela, J.-P. Mikkola, *Appl. Catal. B*, 241 (2019) 41-51. <https://doi.org/10.1016/j.apcatb.2018.09.019>
- [84] J. Sun, W. Cheng, Z. Yang, J. Wang, T. Xu, J. Xin, S. Zhang, *Green Chem.* 16 (2014) 3071-3078. <https://doi.org/10.1039/C3GC41850B>
- [85] C. Yang, M. Liu, J. Zhang, X. Wang, Y. Jiang, J. Sun, *Mol. Catal.* 450 (2018) 39-45. <https://doi.org/10.1016/j.mcat.2018.02.018>

- [86] M. Alves, B. Grignard, R. Méreau, C. Jerome, T. Tassaing, C. Detrembleur, *Catal. Sci. Technol.* 7 (2017) 2651-2684. <https://doi.org/10.1039/C7CY00438A>
- [87] M. Aresta, A. Dibenedetto, A. Angelini, *Chem. Rev.* 114 (2013) 1709-1742. <https://doi.org/10.1021/cr4002758>
- [88] J. Wu, J. A. Kozak, F. Simeon, T. A. Hatton, T. F. Jamison, *Chemical Science* 5 (2014) 1227. <http://doi.org/10.1039/c3sc53422g>

## **Supplementary Data**

### **A non-metal Acen-H catalyst for the chemical fixation of CO<sub>2</sub> into cyclic carbonates under solvent- and halide-free mild reaction conditions**

Zhongxiao Yue <sup>a</sup>, Manoj Pudukudy <sup>a,b</sup>, Shiyu Chen<sup>a</sup>, Yi Liu <sup>a</sup>, Wenbo Zhao <sup>a</sup>, Junya Wang <sup>b</sup>,  
Shaoyun Shan <sup>a,\*</sup>, Qingming Jia <sup>a,1</sup>

<sup>a</sup> *Faculty of Chemical Engineering, Kunming University of Science and Technology, Kunming, Yunnan, 650500, China*

<sup>b</sup> *Faculty of Environmental Science and Engineering, Kunming University of Science and Technology, Kunming, Yunnan, 650500, China*

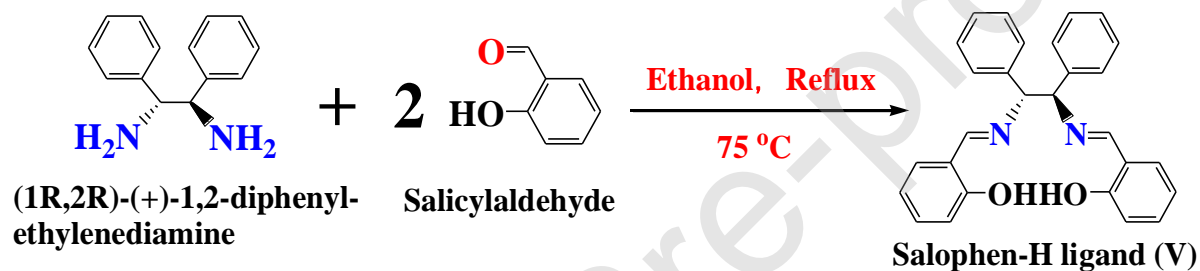
\*Email: [huagong327@163.com](mailto:huagong327@163.com); [shansy411@163.com](mailto:shansy411@163.com)

(1 Deceased author, Date of Death: 25<sup>th</sup> November 2019)

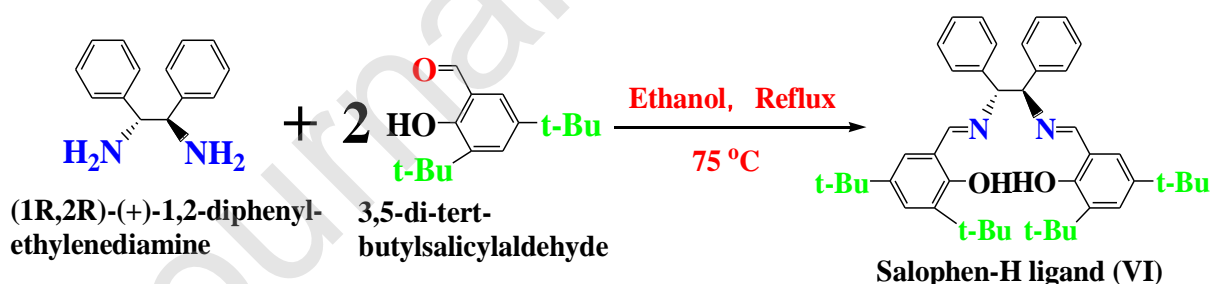
#### **1. Synthesis of homogeneous Salophen-H ligands (V) and (VI)**

A single step method was used to prepare the Salophen-H ligand (V). A solution of (1R,2R)-(+)-1,2-diphenylethylenediamine (1.0615 g, 0.005 mol) in absolute ethanol (60 mL) was taken in a two-neck round bottom flask (250 mL) and placed in an oil bath with magnetic stirring. A reflux condenser and a separation funnel were then placed on the above-mentioned flask. Next, salicylaldehyde (1.05 mL, 0.010 mol) was dissolved in absolute ethanol (50 mL). The reaction temperature of the first mixture was increased to 75 °C, the prepared ethanolic solution of salicylaldehyde was slowly added into the above solution, stirred and heated at 75 °C. The reaction

was performed for 24 h unless it was noted separately. When the reaction was completed, it was cooled to room temperature, and the mixture in the reaction vessel was then allowed to cool in an ice bath. The resultant yellow crystal was filtered by sand core funnel, and washed with ethanol for several times. Finally, the formed product was transferred into a vacuum oven and dried at 55 °C for 6 h. The product obtained in the form of a bright yellow crystal was named as Salophen-H ligand (V) (Fig. 5). For the synthesis of Salophen-H ligand (VI), the experiment was performed with the addition of 3,5-di-tert-butylsalicylaldehyde (2.3433 g, 0.010 mol) instead of salicylaldehyde [39]. The product was obtained in the form of light-yellow powder. A schematic representation of the synthesis route of Salophen-H ligands, (V) and (VI) is shown in Scheme. S1 and Scheme. S2 respectively.



**Scheme S1.** Schematic representation of the synthesis of metal-free Salophen-H ligand (V).



**Scheme S2.** Schematic representation of the synthesis of metal-free Salophen-H ligand (VI).

## 2. Structural characterization of the prepared samples

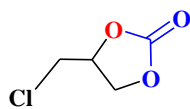
**2.1 Acen-H catalyst:**  $^1\text{H}$  NMR (600 MHz,  $\text{CDCl}_3$ ) [45, 51, 52]  $\delta$  7.39-7.19 (m, 5H, H6-H10), 4.72 (s, 1H, H3), 2.17 (s, 3H, H1), 2.12 (d,  $J = 1.7$  Hz, 3H, H4), 1.54 (s, 1H, H5).  $^{13}\text{C}$  NMR (151 MHz,

CDCl<sub>3</sub>) [51, 54, 56]  $\delta$  162.95 (C4), 143.34 (C7), 128.67 (C10), 127.47 (C9/C11), 126.53 (C8/C12), 77.28-76.85 (CDCl<sub>3</sub>), 61.87 (C6), 30.55 (C3), 23.23 (C1), 15.33 (C5). FT-IR (neat, cm<sup>-1</sup>) [44-47]:  $\nu$  3202 (-OH), 1618 (C=N), 1492 (C-N), 1452 (C=C), 1025 (C-O), 696 (-OH). Elemental analysis: calculated for C<sub>24</sub>H<sub>28</sub>N<sub>2</sub>O<sub>2</sub> (376.5, 4.933 mg): C 76.56, H 7.50, N 7.44 %; found: C 76.72, H 7.48, N 7.20 %.

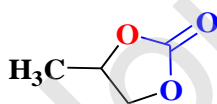
**2.2 (1R,2R)-(+)-1,2-diphenylethylenediamine:** <sup>1</sup>H NMR (600 MHz, CDCl<sub>3</sub>) [51]  $\delta$  7.32-7.22 (m, 5H, H3-H7), 4.11 (s, 1H, H1), 1.63 (s, 2H, H2). <sup>13</sup>C NMR (151 MHz, CDCl<sub>3</sub>) [51]  $\delta$  143.33 (C2), 128.26 (C5), 127.07 (C4/C6), 126.92 (C3/C7), 77.26-74.63 (CDCl<sub>3</sub>), 61.88 (C1). FT-IR (neat, cm<sup>-1</sup>) [44, 47]:  $\nu$  3374 (-NH<sub>2</sub>), 3352 (-NH<sub>2</sub>), 1492 (C-N).

**2.3 2,4-pentanedione:** <sup>1</sup>H NMR (600 MHz, CDCl<sub>3</sub>) [48-50]  $\delta$  5.47 (d,  $J$  = 1.9 Hz, 1H, H2'), 3.56 (d,  $J$  = 1.4 Hz, 2H, H2), 2.19 (d,  $J$  = 2.1 Hz, 3H, H1), 1.99 (s, 3H, H1'). <sup>13</sup>C NMR (151 MHz, CDCl<sub>3</sub>) [55]  $\delta$  202.16 (C2), 191.18 (C2'), 100.40 (C3'), 77.27-75.23 (CDCl<sub>3</sub>), 58.43 (C3), 30.82 (C1), 24.75 (C1'). FT-IR (neat, cm<sup>-1</sup>) [48],  $\nu$  1720 (C=O), 1622 (C=O).

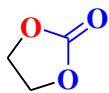
### **3. Spectral characteristics of the cyclic carbonates shown in Table 3 [40, 88]**



**3-Chloropropylene Carbonate:** <sup>1</sup>H NMR (600 MHz, CDCl<sub>3</sub>)  $\delta$  5.06 (tdd,  $J$  = 8.1, 3.8, 2.3 Hz, 1H, OCH), 4.63 (qd,  $J$  = 8.4, 5.4 Hz, 1H, OCH<sub>2</sub>), 4.43 (dtd,  $J$  = 14.3, 7.9, 7.4, 2.5 Hz, 1H, OCH<sub>2</sub>), 3.87 (ddt,  $J$  = 12.5, 4.3, 2.2 Hz, 1H, CH<sub>2</sub>Cl), 3.77 (ddt,  $J$  = 12.4, 8.2, 3.5 Hz, 1H, CH<sub>2</sub>Cl). <sup>13</sup>C NMR (151 MHz, CDCl<sub>3</sub>)  $\delta$  154.57 - 154.51 (C=O), 74.53 - 74.48 (OCH), 66.99 (OCH<sub>2</sub>), 44.26 - 44.06 (CH<sub>2</sub>Cl). FT-IR (neat, cm<sup>-1</sup>):  $\nu$  3746, 3000, 2921, 1798 (C=O), 1277, 1165, 1069, 757 (C-Cl).

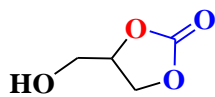


**Propylene Carbonate:** <sup>1</sup>H NMR (600 MHz, CDCl<sub>3</sub>)  $\delta$  4.88 (dddt,  $J$  = 12.0, 8.0, 6.2, 3.0 Hz, 1H, OCH), 4.58 (tt,  $J$  = 8.2, 2.0 Hz, 1H, OCH<sub>2</sub>), 4.05 (ddt,  $J$  = 8.7, 7.2, 1.9 Hz, 1H, OCH<sub>2</sub>), 1.50 (dt,  $J$  = 5.4, 2.4 Hz, 2H, CH<sub>3</sub>). <sup>13</sup>C NMR (151 MHz, CDCl<sub>3</sub>)  $\delta$  155.22 (C=O), 73.74 (OCH), 70.78 (OCH<sub>2</sub>), 19.41 (CH<sub>3</sub>). FT-IR (neat, cm<sup>-1</sup>):  $\nu$  3740, 2985, 2923 (CH<sub>2</sub>), 1788 (C=O), 1385, 1348, 1177, 1042, 778.

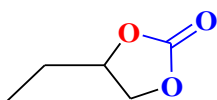


**Ethylene carbonate:**  $^1\text{H}$  NMR (600 MHz,  $\text{CDCl}_3$ )  $\delta$  4.53 (d,  $J = 1.2$  Hz, 2H,  $\text{OCH}_2$ ).

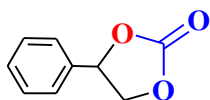
$^{13}\text{C}$  NMR (151 MHz,  $\text{CDCl}_3$ )  $\delta$  155.55 (C=O), 64.67-64.66 ( $\text{OCH}_2$ ). FT-IR (neat,  $\text{cm}^{-1}$ ):  $\nu$  3672, 2980, 2893, 1810 (C=O), 1394, 1237, 1066.



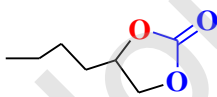
**3-Hydroxypropylene Carbonate:**  $^1\text{H}$  NMR (600 MHz, Deuterium Oxide)  $\delta$  5.37 - 4.85 (m, 1H, OCH), 4.64 - 4.49 (m, 1H,  $\text{OCH}_2$ ), 4.45 - 4.14 (m, 1H,  $\text{OCH}_2$ ), 3.94 - 3.75 (m, 1H,  $\text{CH}_2\text{OH}$ ), 3.73 - 3.57 (m, 1H,  $\text{CH}_2\text{OH}$ ), 3.48 - 3.42 (m, 1H, OH).  $^{13}\text{C}$  NMR (151 MHz, Deuterium Oxide)  $\delta$  157.73 (C=O), 78.03 (OCH), 66.81 ( $\text{OCH}_2$ ), 60.89 ( $\text{CH}_2\text{OH}$ ). FT-IR (neat,  $\text{cm}^{-1}$ ):  $\nu$  3500 (OH), 2994, 2948, 1783 (C=O), 1398, 1262 (OH), 1176, 1069 ( $\text{CH}_2\text{-OH}$ ), 855, 774.



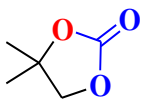
**1,2-Butene Carbonate:**  $^1\text{H}$  NMR (600 MHz,  $\text{CDCl}_3$ )  $\delta$  4.69 - 4.60 (m, 2H, OCH), 4.54 - 4.45 (m, 2H,  $\text{OCH}_2$ ), 4.09 - 3.99 (m, 2H,  $\text{OCH}_2$ ), 1.79 - 1.72 (m, 1H,  $\text{CH}_2\text{CH}_3$ ), 1.75 - 1.66 (m, 1H,  $\text{CH}_2\text{CH}_3$ ), 1.02 - 0.89 (m, 27H,  $\text{CH}_3$ ).  $^{13}\text{C}$  NMR (151 MHz,  $\text{CDCl}_3$ )  $\delta$  155.23 (C=O), 78.10 (OCH), 69.07 ( $\text{OCH}_2$ ), 26.86 ( $\text{CH}_2$ ), 8.45 ( $\text{CH}_3$ ). FT-IR (neat,  $\text{cm}^{-1}$ ):  $\nu$  3672, 2974, 1795 (C=O), 1379, 1288, 1171, 1057, 772, 673.



**Styrene Carbonate:**  $^1\text{H}$  NMR (600 MHz,  $\text{CDCl}_3$ )  $\delta$  7.75 - 7.35 (m, 5H, Ar-H), 5.75 - 5.57 (m, 1H, OCH), 4.89 - 4.70 (m, 1H,  $\text{OCH}_2$ ), 4.46 - 4.16 (m, 1H,  $\text{OCH}_2$ ).  $^{13}\text{C}$  NMR (151 MHz,  $\text{CDCl}_3$ )  $\delta$  154.96 (C=O), 135.86 (ArC), 129.74 (ArCH), 129.24 (ArCH), 125.96 (ArCH), 78.06 (OCH), 71.22 ( $\text{OCH}_2$ ). FT-IR (neat,  $\text{cm}^{-1}$ ):  $\nu$  3740, 3041 (Ar-H), 2991, 1801 (C=O), 1389, 1283, 1162, 1061, 873, 759, 686.



**1,2-hexene Cyclocarbonate:**  $^1\text{H}$  NMR (600 MHz,  $\text{CDCl}_3$ )  $\delta$  4.69 (tt,  $J = 7.8$ , 4.2 Hz, 0H, OCH), 4.54 - 4.48 (m, 0H,  $\text{OCH}_2$ ), 4.05 (dd,  $J = 8.9$ , 7.4 Hz, 0H, ,  $\text{OCH}_2$ ), 1.99 (s, 0H,  $\text{OCHCH}_2$ ), 1.84 - 1.75 (m, 0H,  $\text{OCHCH}_2\text{CH}_2$ ), 1.77-1.66(m, 0H,  $\text{CH}_2\text{CH}_3$ ), 0.90 (t,  $J = 7.7$  Hz, 3H,  $\text{CH}_3$ ).  $^{13}\text{C}$  NMR (151 MHz,  $\text{CDCl}_3$ )  $\delta$  155.15 (C=O), 77.10 (OCH), 69.41 ( $\text{OCH}_2$ ), 33.52 ( $\text{OCHCH}_2$ ), 26.42( $\text{OCHCH}_2\text{CH}_2$ ), 22.23 ( $\text{CH}_2\text{CH}_3$ ), 13.77 ( $\text{CH}_3$ ). FT-IR (neat,  $\text{cm}^{-1}$ ):  $\nu$  3746, 2937, 2869, 1796 (C=O), 1466, 1380, 1283, 1171, 1065, 759, 673.



**2-Methylpropylene Carbonate:**  $^1\text{H}$  NMR (600 MHz,  $\text{CDCl}_3$ )  $\delta$  4.12 (d, 2H,  $\text{OCH}_2$ ), 1.47 (d,  $J = 3.6$  Hz, 6H,  $2 \times \text{CH}_3$ ).  $^{13}\text{C}$  NMR (151 MHz,  $\text{CDCl}_3$ )  $\delta$  154.68 (C=O), 81.80 ( $\text{OC}(\text{CH}_3)_2$ ), 75.35 ( $\text{OCH}_2$ ), 25.96 ( $2 \times \text{CH}_3$ ). FT-IR (neat,  $\text{cm}^{-1}$ ):  $\nu$  3740, 2974, 2924, 1796 (C=O), 1379, 1283, 1126, 1057, 778, 673.

\*\*\*\*\*

Journal Pre-proof